iScience

CellPress
OPEN ACCESS

Review

Electrochemical approaches for selective recovery of critical elements in hydrometallurgical processes of complex feedstocks

Kwiyong Kim,[1] Riccardo Candeago,[1] Guanhe Rim,[2,3] Darien Raymond,[1] Ah-Hyung Alissa Park,[2,3] and Xiao Su[1,*]

SUMMARY

Critical minerals are essential for the ever-increasing urban and industrial activities in modern society. The shift to cost-efficient and ecofriendly urban mining can be an avenue to replace the traditional linear flow of virgin-mined materials. Electrochemical separation technologies provide a sustainable approach to metal recovery, through possible integration with renewable energy, the minimization of external chemical input, as well as reducing secondary pollution. In this review, recent advances in electrochemically mediated technologies for metal recovery are discussed, with a focus on rare earth elements and other key critical materials for the modern circular economy. Given the extreme heterogeneity of hydrometallurgically-derived media of complex feedstocks, we focus on the nature of molecular selectivity in various electrochemically assisted recovery techniques. Finally, we provide a perspective on the challenges and opportunities for process intensification in critical materials recycling, especially through combining electrochemical and hydrometallurgical separation steps.

INTRODUCTION

Critical raw elements are essential in our modern society, being ubiquitous in all areas of industry, especially renewable energy technologies and metallurgical manufacturing, and in everyday life, for example in electronic devices, phones, and electric vehicles. Global accessibility to these important resources poses a major challenge, due to their rapidly increasing demand, and ever-decreasing supply. The global use of critical resources is expected to double between 2010 and 2030, following predicted economic growth (European Commission, 2018), thus placing serious pressure related to sustainable supply chains and environmental issues. The US Department of Energy (DOE) "Critical Materials Strategy" report assessed 16 elements based on their criticality to the clean energy industry and associated supply risk (U.S. Department of Energy, 2011). In addition, the European Commission recently carried out an assessment of 83 raw materials and identified 30 elements as critical, based on economic significance and supply risks (European Commission, 2020), with the major critical materials highlighted in Figure 1.

In particular, the ongoing technological evolution has resulted in a rapidly growing generation of waste electrical and electronic equipment (WEEE) (Işıldar et al., 2018). It has been reported that over 40 Mt of electronic waste have been generated every year since 2014, with only 20% being recycled, and with a projected increase to over 52 Mt in 2021 (Figure 2) (Baldé et al., 2017; Gollakota et al., 2020). Thus, the high metal content in WEEEs makes them a valuable, secondary raw stream for urban mining and recycling. In addition to value-added benefits in recycling, our current reliance of a great deal of commodities and raw materials on virgin sources poses serious environmental risks (Zeng et al., 2018). Owing to a variety of toxic substances in electronic devices, WEEE leads to significant harmful effects on the environment and human health (Baldé et al., 2017). Therefore improving the efficiency of recovery of metal from either primary mining processing or from secondary waste, as well as sustainable urban mining/recycling, is of utmost importance to both the economy and environment, enabling the transition from a traditional linear supply chain that is described as "take, make, and dispose" to a closed loop for a sustainable circular economy (Gaustad et al., 2018).

In the current recycling trains, an initial stage of energy-intensive shredding and physical separation takes place before the separation of ferrous/non-ferrous metal streams and non-metallic fractions (Hsu et al.,

[1]Department of Chemical and Biomolecular Engineering, University of Illinois at Urbana-Champaign, Urbana, IL 61801, USA

[2]Department of Earth and Environmental Engineering, Department of Chemical Engineering, Columbia University, New York, NY 10027, USA

[3]Lenfest Center for Sustainable Energy, The Earth Institute, Columbia University, New York, NY 10027, USA

*Correspondence: x2su@illinois.edu

https://doi.org/10.1016/j.isci.2021.102374

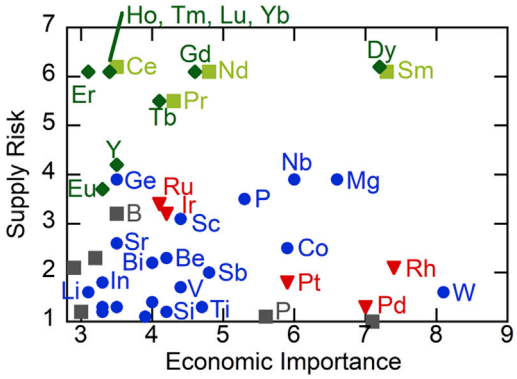

Figure 1. Assessment of material criticality based on economic importance and supply risk

Dark green: heavy rare earths, light green: light rare earths, red: platinum group metals, dark gray: non-metallic elements in supply risk, blue: other metals in supply risk within criticality zone of high economic importance (≥2.8) and supply risk (≥1). Adapted with permission (European Commission, 2020).

2019). Subsequently, the metal-rich streams are subjected to pyrometallurgical or hydrometallurgical refining. Because of intrinsic limitations of conventional pyrometallurgical processes, e.g., large energy input, environmental hazard, the need of additional processing, lack of selectivity, and high capital cost, hydrometallurgical methods have been welcomed as a more sustainable alternative compared with pyrometallurgical routes (Sethurajan et al., 2019; Tunsu and Retegan, 2016). In hydrometallurgical refining processes, leach liquor or contaminated water streams from acid/base leaching have to be treated with separation techniques such as solvent extraction, ion exchange, precipitation, adsorption, and electrochemical methods (Sethurajan et al., 2019). The state-of-the-art for hydrometallurgical recoveries have been presented in several recent review articles and cover a broad range of different technologies (Hsu et al., 2019; Sethurajan et al., 2019; Tunsu and Retegan, 2016)

Recently, remarkable attention has been paid to electrochemical metal recovery for the purpose of enabling circular economy (Chernyshova et al., 2020; Jin and Zhang, 2020). Contrary to traditional recovery techniques, which are chemically intensive and often require large pH or thermal swing (Ambaye et al., 2020; Tunsu and Retegan, 2016), electrochemical methods offer a modular approach as an alternative of traditional chemical/thermal swing-based separations (Su, 2020a). The main challenge is selectivity; because the target metal ions are usually minority components in the presence of excess competing species in the primary mining or secondary waste stream, there have been extensive efforts to ensure selective recovery in dilute streams, and electrochemically mediated technologies offer a desirable platform tackling this selectivity issue (Gamaethiralalage et al., 2021; Su, 2020a).

In this review, we present recent advances in electrochemically mediated metal recovery technologies, as well as its close synergistic connection with hydrometallurgical approaches. We place a special focus on hydrometallurgical and electrochemical approaches that can benefit critical materials recycling, especially for rare earth elements and other valuable transition metals. We also seek to provide insights into the mechanisms and applications for different electrochemical techniques, namely, electrodeposition, electrosorption, electrodialysis, and electrocoagulation (EC), and highlight the need for the design of molecular selectivity in the development of next-generation electrochemical recovery. Finally, we discuss the challenges and opportunities for electrochemically assisted recovery techniques, both at an interfacial electrode level, and from a process design perspective.

HYDROMETALLURGY FOR THE LEACHING AND RECOVERY OF METALS

Principles of hydrometallurgical leaching

Hydrometallurgical processes for the recovery of critical metals from ores and waste streams usually proceed through two main stages: leaching and recovery. In hydrometallurgical leaching, the metal content in a solid phase is chemically reacted and transferred into liquid (aqueous) matrix. After the leaching step, metals of interest are recovered from the leachates using appropriate separation technologies, including non-electrochemical techniques (e.g., cementation, solvent extraction, adsorption, ion exchange), or new approaches such as electrochemically mediated recovery (Figure 3).

The majority of the chemical leaching studies on electronic wastes has been focused on the extraction of Cu and Au, which are the most abundant and valuable element, respectively, from waste printed circuit boards

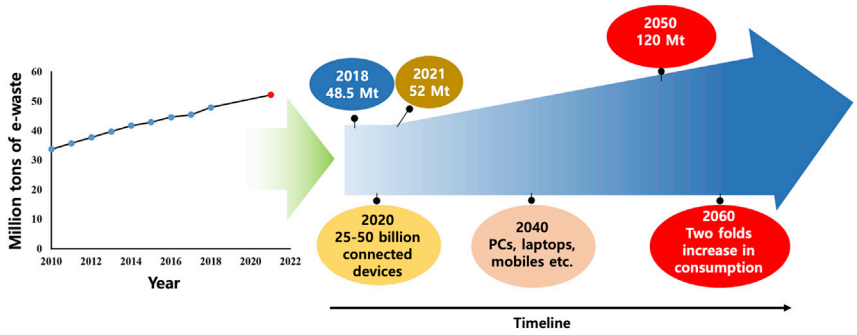

Figure 2. Increasing trend of the generation of worldwide electronic wastes
Adapted from (Gollakota et al., 2020).

(WPCBs) (Ajiboye et al., 2019; Behnamfard et al., 2013; Birloaga et al., 2013; Koyama et al., 2006; Li et al., 2020a; Mecucci and Scott, 2002; Yousefzadeh et al., 2020). Table 1 describes the most common solvents being used for the chemical leaching of Cu and Au, including the overall chemical reactions and potential drawbacks.

Some of the most common leaching agents in hydrometallurgical processes are mineral and organic acids, cyanide, aqua regia, thiosulfate, and thiourea. First, the acid leaching method has often been used due to its high leaching rate. In particular, nitric acid (HNO_3) leaching solutions have been commonly used for the extraction of Cu, Pb, and Sn from WPCBs (Kumari et al., 2016; Mecucci and Scott, 2002; Neto et al., 2016). Sulfuric acid (H_2SO_4) has also been proved to be effective for the hydrometallurgy of WPCBs, when used with hydrogen peroxide (H_2O_2) as an oxidant (Silvas et al., 2015; Xiao et al., 2013; Yang et al., 2011). The solvent containing H_2SO_4 and H_2O_2 showed one of the highest leaching efficiencies of Cu from WPCBs, reaching as high as 100% Cu leaching in 4 h from WPCBs (Silvas et al., 2015). Although a high concentration of a strong acid could provide efficient leaching of metals such as Cu, the leaching solution containing Cu could not be directly used in the subsequent step of the electrodeposition of Cu, because the highly acidic condition inhibited the deposition of Cu (Maguyon et al., 2012).

Other strong leaching systems, such as aqua regia (a 1:3 molar mixture of HNO_3 and HCl) (Elomaa et al., 2017; Petter et al., 2015) and cyanide (Fleming, 1992; Montero et al., 2012), have also been investigated to extract inert precious metals (e.g., Au) from WPCBs. Aqua regia has shown highly efficient extraction behaviors of Cu, Au, and Ag from WPCBs, but unfortunately, it has severe drawbacks such as environmental and public health concerns, high corrosiveness, volatility, toxic emissions, and low selectivity (Hsu et al., 2019). The cyanide leaching method, which was developed for gold mining, has been widely commercialized for over 100 years (Behnamfard et al., 2013) based on its great leaching efficiency and lower cost when compared with other conventional solvents (Akcil et al., 2015). However, the most well-developed cyanide leaching technology has also been gradually phased out due to a number of health and environmental issues including extremely high toxicity and corrosiveness (Fleming, 1992; Hsu et al., 2019).

State-of-the-art leaching processes for critical metal recovery

Owing to severe drawbacks of strong acid and cyanide leaching techniques in terms of toxicity and environmental threats, less hazardous hydrometallurgical routes utilizing chelating agents including thiosulfates (Fotoohi and Mercier, 2014; Ha et al., 2010, 2014; Jeon et al., 2018; Kasper et al., 2018; Oh et al., 2012; Tripathi et al., 2012) and thiourea (Behnamfard et al., 2013; Birloaga et al., 2013; Gurung et al., 2013; Jing-ying et al., 2012) have been explored to extract precious metals from WEEE. The potential of thiosulfate solutions was confirmed, showing 90% Au extraction from WPCBs in mobile phones in the presence of copper salt, thiosulfate, and ammonia (Fotoohi and Mercier, 2014; Ha et al., 2010). Another leaching study on WPCBs showed that 95% Au and 100% Ag were extracted with the thiosulfate solution, 0.2 M $(NH_4)_2S_2O_3$, 0.02 M $CuSO_4$, and 0.4 M NH_4OH, within 48 and 24 h, respectively (Oh et al., 2012). Very high extents of Au (86%) and Ag (71%) extraction were also achieved with a thiourea leaching solution when ferric ion was used as an oxidant (Behnamfard et al., 2013). However, both hydrometallurgical processes utilizing thiosulfate and thiourea required large amounts of reagent due to slow kinetics of thiosulfate and poor stability of thiourea (Birloaga et al., 2013; Gurung et al., 2013; Hsu et al., 2019; Jing-ying et al.,

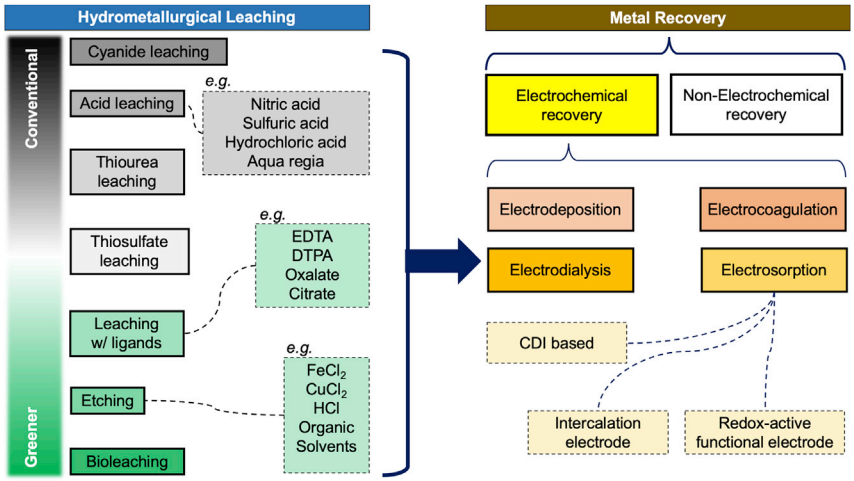

Figure 3. Hydrometallurgical leaching processes followed by critical materials recovery techniques

2012). Thus, the process development and scale-up of these hydrometallurgical systems with reduced hazards are still challenging.

To develop a greener hydrometallurgical pathway for precious metal recovery from WEEE as well as Cu leaching, a supercritical carbon dioxide ($scCO_2$)-facilitated treatment technology combined with an acid leaching process has been proposed (Calgaro et al., 2015; Hsu et al., 2019, Hsu et al., 2020; Peng and Park, 2020). The $scCO_2$ significantly enhanced Cu extraction resulting in 90% Cu recovery within 20 min (Calgaro et al., 2017). The mechanistic study showed that $scCO_2$ interacted with metal layers, fiberglass, and polymers in WPCBs and led to chemical and physical changes in WPCBs that enhanced Au recovery and Cu leaching (Hsu et al., 2020; Peng and Park, 2020). Thus, the overall acid requirement for metal extraction from WPCBs was significantly reduced. As the $scCO_2$-based technology can directly work with untreated WPCBs, the thermal pretreatment step (e.g., two-step pyrolysis) of halogen-containing polymeric compounds in WPCBs, such as Br and Cl in phenols and flame retardants (Gamse et al., 2000), can be potentially eliminated. Therefore, toxic gaseous emissions (e.g., HBr) from the WPCB treatment process may also be significantly reduced. Furthermore, the addition of a co-solvent (e.g., ethanol) to the $scCO_2$-based solvent system may allow the decomposition, extraction, and separation of Br and Cl compounds via a safer route (Fleming, 1992; Hong-Chao et al., 2006). This innovative hydrometallurgical approach is also one of the unique emerging technologies because it utilizes the most significant greenhouse gas, CO_2.

Peng and Park (2020) reported that $scCO_2$-based solvent could induce synergistic physical and chemical alterations of the polymer-metal matrix in WPCBs resulting in enhanced metal extraction behaviors, while allowing Au recovery via hydrometallurgical delamination. This technology is innovative because Au could be recovered as solids instead of dissolved species, as shown in Table 1. The selective recovery of solid Au would simplify the downstream metal recovery process and minimize the loss of Au. Based on their findings, a two-step $scCO_2$-based WPCB treatment process was proposed, as illustrated in Figure 4. In the first stage, the $scCO_2/H_2SO_4$ solvent extracts Ca and Al from the calcium-silicate-bearing fiberglass within WPCBs, creating unique inner porous structures for selective leaching of Ni. As Ni was leached out, Au, which was mostly distributed on the surface of WPCBs, is released into the liquid phase as solids, through a process referred to as now hydrometallurgical delamination. During the second stage, the Cu is effectively extracted using a conventional H_2SO_4/H_2O_2 (acid/oxidant) solvent, but its concentration and the quantity required for metal leaching can be significantly reduced because the WPCBs from the first stage are now highly reactive.

ELECTROCHEMICAL SEPARATIONS FOR SELECTIVE RECOVERY

After the leaching step, metals of interest need to be recovered from the leachates selectively. In view of the reagent- and energy-intensive nature of the most practiced recovery processes (e.g., solvent extraction, ion exchange, adsorption, and precipitation) and the extreme heterogeneity of hydrometallurgical streams, the development of effective, selective, and sustainable recovery is recognized as one of

Table 1. Solvents used in hydrometallurgy of Cu and Au

Leaching solvent	Example	Overall reactions	Challenges and limitations
Acid	HNO_3	$4HNO_3 + Cu \rightarrow Cu(NO_3)_2 + 2NO_2 + 2H_2O$	Nitric acid would inhibit the downstream electroplating process
Acid + oxidant	H_2SO_4: H_2O_2	$Cu + 2H^+ + H_2O_2 \rightarrow Cu^{2+} + 2H_2O$	Highly corrosive
Mixture acid	Aqua regia	$2Au + 11HCl + 3HNO_3 \rightarrow 2HAuCl_4 + 3NOCl + 6H_2O$	Highly corrosive, metal specificity (targeted toward Cu recovery with chlorides)
Cyanide	NaCN	$4Au + 8CN^- \rightarrow 4Au(CN)_2^- + 4e^-$	Slow leaching rate, harmful wastewater
Thiourea	$CS(NH_2)_2$	$Au + 2CS(NH_2)_2 \rightarrow Au(CS(NH_2)_2)^{2+} + e^-$	Poor stability, high reagent consumption
Thiosulfate	$(S_2O_3)^{2-}$	$Au + 5S_2O_3^{2-} + Cu(NH_3)_4^{2+} \rightarrow Au(S_2O_3)_2^{3-} + Cu(S_2O_3)_3^{5-} + 4NH_3$	High selectivity, but high reagent consumption

Adapted from (Hsu et al., 2019).

significant importance in industry. Electrochemical pathways can provide sustainable options, which, at least in a complementary way, help avoid (1) the intensive use of toxic chemicals, (2) the generation of secondary wastes, or (3) large pH or thermal swings (Jin and Zhang, 2020). The versatile, modular, reversible, and scalable features of electrochemical metal recovery approaches can contribute to the operation with high efficiency and cost effectiveness (Jin and Zhang, 2020). Modulating electrochemical stimuli (e.g., potential, current density) provides a way of controlling electron transfer and Faradaic/non-Faradaic processes in a reversible fashion in electrochemically mediated systems, allowing for designing a technology for metal extraction/recovery with high reversibility, regenerability, Faradaic efficiency, and selectivity (Srimuk et al., 2020). At a higher level, with combination with renewable energy sources, electrochemical processes can enable sustainable and distributed processes for metal recycling.

After the first discovery of metal plating in the 1700s by Beccaria, who discharged a Leyden bottle and used the spark to decompose metal salts (Raub, 1993), extensive progress has been made to recover metals from industrial mining/waste streams. Electro-refining of copper has been carried out by anodic dissolution of impure copper and simultaneous electroplating of pure copper (Grotheer et al., 2006), with careful control of operational parameters for achieving the highest purity of recovered metals. However, a major bottleneck of electrochemical recovery is selectivity in multicomponent mixtures. Metals in natural ores and electronic wastes are not in a pure form and contain a wide range of impurities, with valuable metals often existing as minority ions in the presence of abundant elements. For example, a high Mg/Li ratio—from several tens to hundreds—is reported for a number of major salt lake brines worldwide, which are important for Li^+ recovery (Shi et al., 2019a). Also, Liu et al. reported the heterogeneous nature of the composition of a spent nickel-metal hydride (Ni-MH) battery and lithium-ion battery (LIB): 43% Ni, 6% Co, 3% Mn, and 22% rare earth elements (REEs) (La, Ce, Pr, and Nd) in a spent Ni-MH battery and 4% Li, 21% Co, 3% Ni, and 2% Mn in a spent LIB battery; these examples show real-world selectivity challenges in hydrometallurgical processes (Liu et al., 2019a).

In the following sections, we discuss recent advances in electrochemical metal recovery processes in multicomponent recycling and urban mining. With the special focus on selectivity, we highlight technologies designed to recover critical elements—including energy-critical elements such as cobalt and nickel (Table 3), lithium (Table 4), and REEs (Table 5), by taking advantage of various electrochemical approaches such as electrodeposition, electrosorption, electrodialysis, and electrocoagulation (Figure 5). In addition, we provide insights into electrochemically modulated regeneration enabled by a simple electrochemical swing with minimal change in pH or temperature, which offers a way of up-concentrating target metals for reprocessing and thus is desirable for addressing material criticality.

Electrodeposition

Electrodeposition (electrowinning) is the most traditional electrochemical metal recovery technique, transforming soluble and thus mobile metal ions into immobilized metallic coatings via electrochemical reactions (Figure 5A). Electrodeposition can be carried out in a safe and simple manner using only a simple system composed of an electroplating bath and inert anode and cathode (Paul Chen and Lim, 2005). Electrodeposition has been extensively explored for the recovery of metals since the 1970s (Bennion and Newman, 1972; Scott, 1981), and early efforts have been made for electroplating of metals with rather

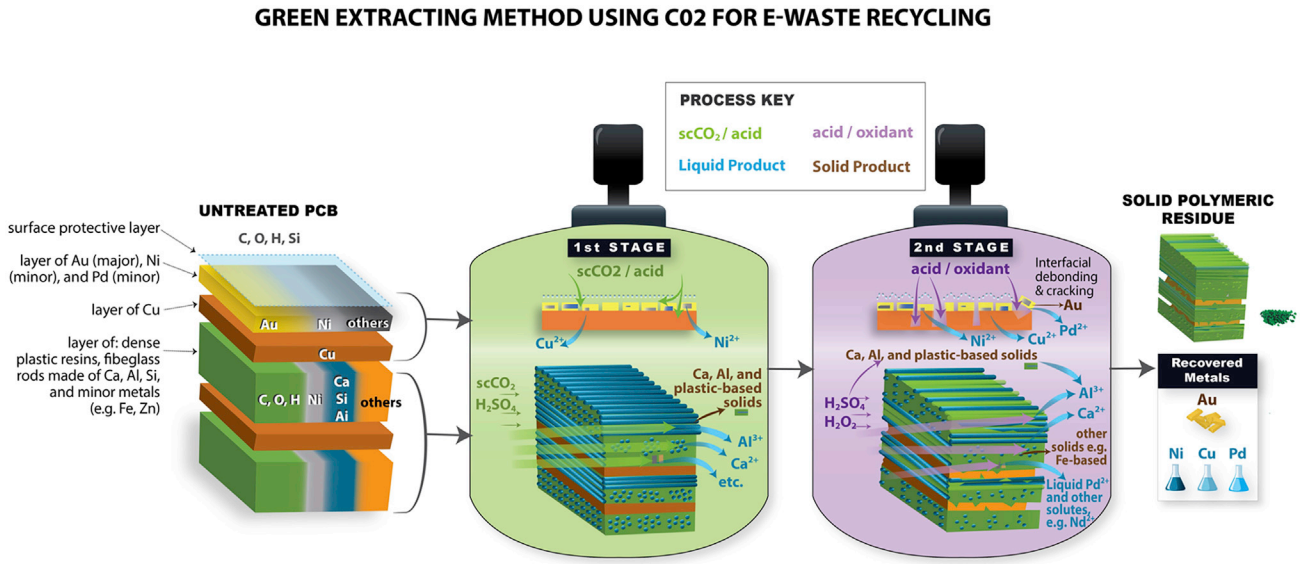

Figure 4. A schematic of the two-stage $scCO_2$-induced printed circuit board (PCB) treatment technology
Reproduced with permission (Peng and Park, 2020). Copyright 2020, Royal Society of Chemistry.

positive redox potentials, such as *copper* and *silver* (0.34 and 0.80 V versus SHE, respectively), which can operate within the electrochemical window of water (Chyan et al., 2003; Kaniyankandy et al., 2007). In particular, copper electrowinning is the most widely investigated due to its enriched composition in electronic wastes (e.g., WPCBs) and its positive standard potential in acid media (Hsu et al., 2019; Mecucci and Scott, 2002; Sun et al., 2015), and for this reason, the electrowinning of other metals is often carried out after copper has been extracted from electronic wastes stream—otherwise, the system would undergo unwanted copper co-deposition (Hsu et al., 2019).

In the case of recovery from dilute solutions, the electrodeposition process is often limited by mass transfer and concentration polarization, so the optimal design of electrochemical reactors is desired. For instance, Jin et al. adopted a cylindrical turbulent cell with improved surface area for facilitating mass transfer, thereby achieving ~93% extraction efficiency of copper and 89.4% current efficiency (Jin et al., 2017). In addition, the optimization of spouted bed electrodes was reported for the recovery of copper from a diluted stream, attaining a high removal efficiency (>99.9%) and space-time yield (86 kg m^{-3} h^{-1}), thanks to improved mass transfer (Martins et al., 2012). In multicomponent streams, the standard reduction potential is one of the most important parameters determining selectivity in the electrodeposition processes; for instance, a careful selection of optimal nucleation potential enabled *cadmium* removal by electrodeposition from a mixture of cadmium, cobalt, and nickel, and ~95% purity cadmium was recovered without serious co-deposition of cobalt and nickel (Armstrong et al., 1996). However, taking into consideration the solution environment (e.g., pH, metal concentration, complexing agent) is also necessary, due to their effect on the thermodynamic reduction potential within real-world liquid streams. For example, Chen et al. attempted a competitive co-deposition of silver and copper for electrochemical recovery and found that the recovery rate of silver was faster than that of copper because the reduction potential of silver is more positive compared with that of copper (Paul Chen and Lim, 2005). When the competitive deposition was further carried out in the presence of silver, copper, and lead, the removal efficiency of lead (>80%) was much higher than the removal efficiency of copper (<20%), which was contrary to expectations based solely on reduction potentials (Paul Chen and Lim, 2005). This result indicates that standard reduction potentials alone do not determine the composition of the deposit; other factors, such as metal concentration, pH, ionic strength, additives, the kind of substrate, chelating agents, mode of electrodeposition (chronoamperometry or chronopotentiometry), applied current signal, temperature, and fluid-dynamic conditions, all work together to determine the characteristics of deposition (Banthia et al., 2017; Ibañez and Fatás, 2005; Kim et al., 2018a; Maarof et al., 2017).

Because the redox potentials of some key elements (e.g., Ga, In, Co, Ni, and Te) are not extremely far away from hydrogen electrode (Table 2) (Haynes, 2012), electroplating of these metals has been attempted in

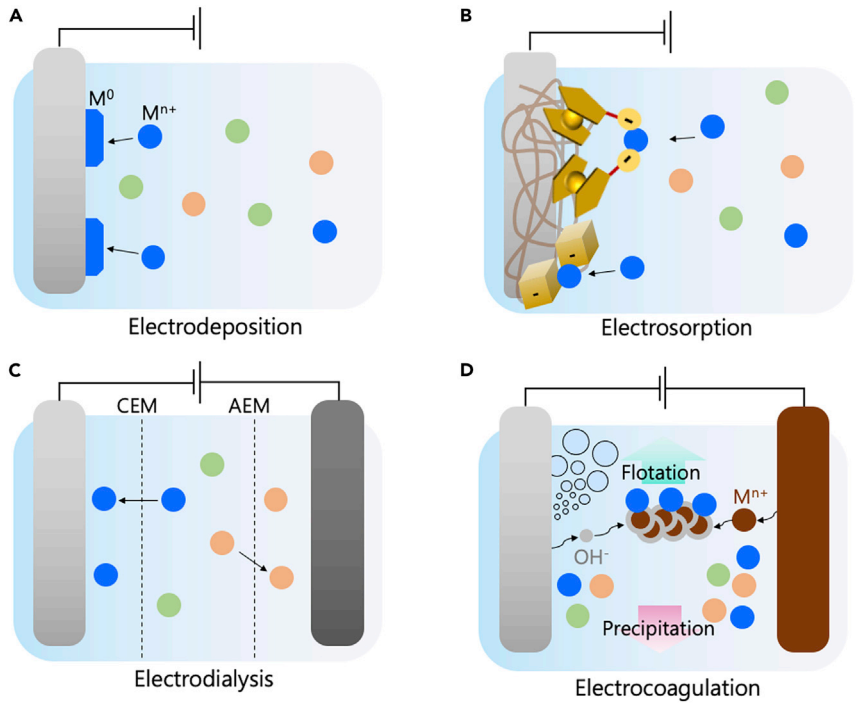

Figure 5. Schematic of different electrochemical processes for selective metal recovery

(A–D) (A) Selective electrodeposition of metal ions on cathodic substrate, (B) selective electrosorption by non-faradaic CDI or pseudocapacitive faradaic electrodes, (C) selective recovery by membrane-based electrodialysis, (D) electrocoagulation processes.

aqueous electrolytes. In such cases, stepwise cathodic electrodeposition offers a way of selective extraction through potentiostatic/galvanostatic operation. The difference in reduction potentials of metal ions determines the feasiblity of a selective electrodeposition process—especially depending on the degree of side reaction taking place (hydrogen evolution) or on the competitive co-deposition of unwanted metals.

Manganese, because of its low equilibrium potential, suffers from interference of side-reactions during electrodeposition, such as hydrogen evolution and co-deposition of other metal cations with higher redox potentials (Padhy et al., 2016). In a single-cation solution of manganese, high current efficiency for manganese deposition was not possible without the use of additives, such as selenium, tellurium, and sulfite compounds in the electrowinning bath (Griškonis et al., 2014; Lu et al., 2014; Sun et al., 2011). Such additives preferentially increased the overpotential of hydrogen evolution, thereby improving the manganese deposition rate (Padhy et al., 2016; Sun et al., 2011). Harris et al. pointed to the existence of metal ion impurities (e.g., Ni, Co, Fe, Cu, and Zn) that can negatively affected the electrowinning of manganese (Harris et al., 1977), and how these impurities must be removed before the electrowinning process (Lu et al., 2014). When electrodeposition was carried out using a solution of dissolved Ni-MH battery, manganese was co-deposited with nickel and cobalt, illustrating challenges in its selective recovery process by Faradaic processes (Santos et al., 2012).

The electrodeposition of *cobalt* or *nickel* has been widely investigated (Table 3), but the selective electrodeposition in their mixture is challenging (Altimari et al., 2019; Cui et al., 1990; Frank and Sumodjo, 2014; Oriňáková et al., 2006). About 55% of the world's cobalt is known to exist in close association with nickel in ores (Sole, 2018), and both metals are employed together in various battery materials, such as $LiNi_xCo_yMn_2O_2$ and Ni-MH battery materials (He et al., 2016; Tzanetakis and Scott, 2004). Owing to the close proximity of the two metals in the periodic table and their very similar standard potentials, selective electrodeposition of the two metals is extremely difficult (Armstrong et al., 1997). After Ni-MH materials were leached, the generated streams containing the mixture of cobalt and nickel were employed in an electrodeposition cell; the composition of cobalt and nickel in the co-deposit was controlled using various operational parameters, such as current density and pH (Santos et al., 2012; Tzanetakis and Scott, 2004).

Table 2. Standard reduction potentials of rare earth and other key elements

	Half reaction	Standard potential (V versus SHE)
Rare earth elements (Haynes, 2012)	$Dy^{3+} + 3e^- \rightarrow Dy$	−2.295
	$Dy^{2+} + 2e^- \rightarrow Dy$	−2.2
	$Tb^{3+} + 3e^- \rightarrow Tb$	−2.28
	$Eu^{3+} + 3e^- \rightarrow Eu$	−1.991
	$Eu^{2+} + 2e^- \rightarrow Eu$	−2.812
	$Nd^{3+} + 3e^- \rightarrow Nd$	−2.323
	$Nd^{2+} + 2e^- \rightarrow Nd$	−2.1
	$Y^{3+} + 3e^- \rightarrow Y$	−2.372
Other key elements (Haynes, 2012)	$Li^+ + e^- \rightarrow Li$	−3.04
	$Mn^{2+} + 2e^- \rightarrow Mn$	−1.185
	$Ga^{3+} + 3e^- \rightarrow Ga$	−0.549
	$In^{3+} + 3e^- \rightarrow In$	−0.3382
	$Co^{2+} + 2e^- \rightarrow Co$	−0.28
	$Ni^{2+} + 2e^- \rightarrow Ni$	−0.257
	$Cu^{2+} + 2e^- \rightarrow Cu$	−0.3419
	$Te^{4+} + 4e^- \rightarrow Te$	0.568
	$TeO_3^{2-} + 3H_2O + 4e^- \rightarrow Te + 6OH^-$	−0.57

Armstrong et al. carried out the electrochemical separation of cobalt and nickel from simulated wastewater using electrodeposition (Armstrong et al., 1997). Cobalt and nickel exhibited no difference in their onset potential for the deposition on a pristine stainless-steel electrode, but pre-deposition of the stainless steel with cobalt facilitated cobalt deposition by lowering nucleation overpotential and increased separation window almost 200 mV. Contrary to the predicted cobalt purity from cyclic voltammetry (CV) of single cations, nevertheless, 100% purity of cobalt could not be obtained (Armstrong et al., 1997). These limitations can be ascribed to the fact that when nickel and cobalt are co-deposited, the presence of cobalt promotes the initiation of nickel nucleation (You et al., 2012). The electrodeposition of cobalt and nickel shows the difficulties in selectively separating two metals with similar reduction potentials.

The electrodeposition of *gallium* and *indium* has been employed for selective separation from solar cell wastes (Gustafsson et al., 2015). The equilibrium potentials of indium and gallium are far enough to enable potentiometric separation (Table 2) (Fogg, 1934; Gustafsson et al., 2015). Copper was first separated from the waste stream by electrodeposition followed by indium electroplating, and the suitable applied potentials for selective electrodeposition were −0.5 V and −0.9 V (versus Ag/AgCl) for copper and indium, respectively, which brought about >98% separation of copper and indium from real solar cell waste (Figure 6) (Gustafsson et al., 2015). Gallium remained in liquid phase, with a small amount of indium remaining in the electrolyte.

Selective recovery of *tellurium* and copper is another key issue. Jin et al. figured out that the reduction potentials of copper and tellurium were close (−0.26 V and −0.38 V versus SCE, respectively), but different speciation in HCl enabled distinct deposition behaviors for selective extraction (Jin et al., 2018). A mass transfer-enhanced turbulent reactor was used for stepwise recovery of copper and tellurium (Figure 7A), achieving >93% purity of tellurium at relatively lower current operation (100 A m^{-2}) followed by >98% purity copper at high current operation (400 A m^{-2}) (Jin et al., 2018). A similar approach employing chloride-rich electrolyte was investigated for selective electrochemical recovery of tellurium from copper; there was a decrease in reduction potential of copper in aqua regia-based solution due to the formation of monovalent copper chloride complexes, and the highest tellurium recovery of 64% was obtained by combined electrodeposition redox replacement and electrowinning processes (Halli et al., 2019) (Figure 7B).

REEs (*dysprosium, terbium, europium, neodymium, and yttrium*) exhibit very negative standard potentials compared with hydrogen evolution (Table 2) and thus are highly reactive in aqueous environments. For this reason, electrodeposition from aqueous electrolyte solutions is not feasible (Sanchez-Cupido et al., 2019). On the other hand, their highly negative potentials have been used as a basis for selective anodic

Table 3. Separation of cobalt from nickel: comparison between different electrochemical techniques based on separation performance metrics

Technique	Co, Ni concentration	Supporting electrolyte composition	Electrode/membrane material	Separation performance metric	Reference
Electrodeposition	0.1 M Co(II) + 0.1 M Ni(II)	Aqueous, 1 M Na_2SO_4	Stainless steel or nickel	90% Co/10% Ni alloy was obtained	(Armstrong et al., 1997)
Electrodeposition	(0.05, 0.20, 0.40 M) Co(II) + 0.5 M Ni(II)	Deep eutectic solvent (choline chloride/ ethylene glycol)	Brass foil	~1.08 Ni over Co separation factor[a]	(You et al., 2012)
Intercalation electrode	1 mg L^{-1} Co(II) + 1 mg L^{-1} Ni(II)	Aqueous	Copper metal hexacyanoferrate	The presence of Ni hindered the removal of Co. Ni removal was not reported	(Long et al., 2020)
Intercalation electrode membrane/ electrodialysis	0.1 M Co(II) + 0.1 M Ni(II)	Aqueous, 0.1 M Na_2SO_4	Mo_6S_8 (Chevrel phase) electrochemical transfer junction	99% Co over Ni selectivity factor[b]	(Guyot et al., 2013)
Electrodialysis	0.01 M Co(II) + 0.01 M Ni(II)	3–6 M HCl solution	Liquid membrane (trialkylbenzylammonium chloride + tri-n-octylamine in 1,2-dichloroethane)	145 Co over Ni separation factor (1:1 Co:Ni), up to 400 (10:1 Co:Ni)[a]	(Sadyrbaeva, 2015)

[a]Separation factor: ratio $(A/B)_{electrode}/(A/B)_{solution}$, or $(A/B)_{strip\ sol}/(A/B)_{feed\ sol}$ for electrodialysis, estimated from Figure 3 (You et al., 2012).
[b]Selectivity factor: ratio n(Co)/(n(Co)+ n(Ni)), where n is the number of moles in the recovery compartment.

dissolution from NdFeB magnets, as well as the selective separation of any co-dissolved non-REEs by cathodic electrodeposition (Prakash et al., 2016; Xu et al., 2020). Given the arduous challenge of plating rare earths in aqueous environment, electrodeposition in nonaqueous electrolytes, and high temperatures, has often been proposed as an effective approach. Selective recovery of Dy from a mixture of $DyCl_3$ and $GdCl_3$ was enabled by electrochemical alloy formation (Mg-Dy) using a reactive magnesium electrode in a eutectic bath of LiCl-KCl at 773 K (Yang et al., 2014); formation of Mg-Dy alloy offered a more energy-efficient platform for selective extraction compared with the direct deposition of metallic Dy; from a 1:1 mixture of $DyCl_3$ and $GdCl_3$, only Dy was extracted without the co-deposition of Gd (Yang et al., 2014). Electrodeposition of REEs has also been investigated using ionic liquids such as ammonium-, pyrrolidinium-, and imidazolium-based electrolytes (Kurachi et al., 2012; Lodermeyer et al., 2006; Sanchez-Cupido et al., 2019). In aqueous environment, because the electroreduction of rare earths into metallic form is almost impossible, a different kind of electrodeposition—formation of oxide on cathode—was reported for selective recovery of rare earths from mixed metal wastes (O'Connor et al., 2018). In the electrochemical system illustrated in Figure 7C, REEs were converted to oxides, assisted by OH^- ions generated from oxygen reduction or water reduction on the cathode. When a multicomponent synthetic stream containing Cu and Eu was injected into multiple stages of filters at different operation voltages, selective separation/ retention of Cu and Eu was achieved with the recovery of 97% and 65% for Cu and Eu, respectively (O'Connor et al., 2018).

Owing to the reactivity of *lithium* with water, most of the lithium electrodeposition studies (e.g., lithium metal anode in battery applications) have been investigated in non-aqueous electrolyte (Sun et al., 2020). To recover lithium ions from aqueous streams, researchers have used lithium-ion-conducting glass-ceramics ($Li_{2+2x}Zn_{1-x}GeO_4$ or $Li_{1+x+y}Ti_{2-x}Al_xP_{3-y}Si_yO_{12}$), which separate an aqueous compartment from an organic electrolyte and thus protect deposited lithium from the exposure to the aqueous electrolyte (Bae et al., 2016; Kim et al., 2018a, 2018b; Wang and Zhou, 2010). The lithium-ion-conducting glass-ceramics allow for the migration of lithium ions only, without the passage of other cations (e.g., Na, Mg, Ca, and K) and the permeation of water (Hoshino, 2015; Kim et al., 2018b). The concept of recovering lithium in the form of high-purity metal film has been proposed using this ceramic-type separator. Bae et al. designed a three-compartment cell to achieve a waste-to-lithium recovery approach (Bae et al., 2016); lithium ions from spent cathodes such as $LiFePO_4$, $LiMn_2O_4$, and $LiNi_{1/3}Co_{1/3}Mn_{1/3}O_2$ were transferred through the ceramic electrolyte from the aqueous waste streams to the non-aqueous Li-harvesting compartment,

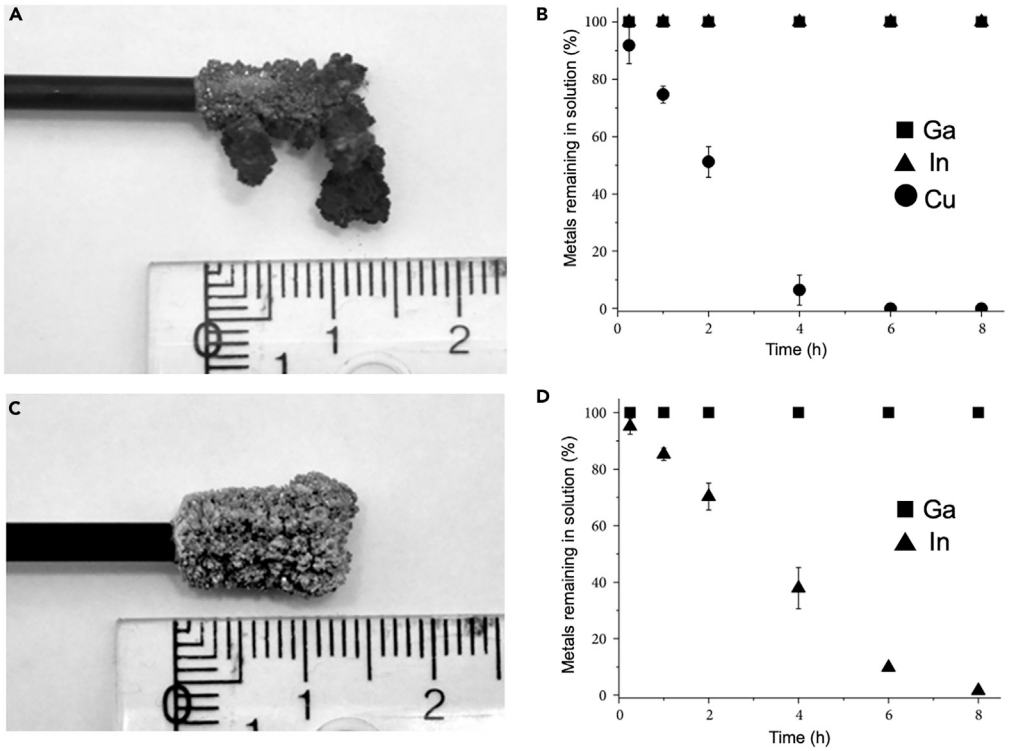

Figure 6. Separation Cu, In, and Ga

(A and B) Selective electrodeposition of Cu. (A) Electroplated Cu from a synthetic solution of 0.25 M Cu, In, Ga in 1 M HCl at −0.5 V (versus Ag/AgCl). (B) Relative concentrations of Cu, In, and Ga in the liquid electrolyte as a function of time. (C and D) Selective electrodeposition of In. (C) Electroplated In at −0.9 V (versus Ag/AgCl) from Cu-depleted electrolyte after Cu electroseparation. (D) Relative concentration of In and Ga in the liquid electrolytes as a function of time. Reproduced with permission (Gustafsson et al., 2015). Copyright 2015, Anna M. K. Gustafsson et al.

thereby being stored in the form of metallic lithium by electrodeposition. Then, in a recycling compartment, the harvested metallic lithium was discharged and reconverted into valuable precursors such as LiOH or Li_2CO_3 with high purity (~99%) (Table 4). A similar approach of using the lithium-ion-conducting glass-ceramic was also reported by different authors (Mashtalir et al., 2018), achieving a high purity of lithium (>99.9%), but the study was not carried out in the presence of competing ions. Nevertheless, considering the high rejection of lithium-ion conducting ceramics against other cations, this approach would offer a way of selective recovery via combined deposition and ion-specific membrane dialysis.

Electrosorption

Electrical field-assisted adsorption is referred to as electrosorption (Su and Hatton, 2016, 2017a). When applying a potential difference, charged species (e.g., ions or charged colloids) migrate to the polarized electrode with opposite charge and are separated from the liquid phase (Figure 5B). Capacitive deionization (CDI) is a fundamental electrosorption platform wherein ions accumulate in the electrical double layer, and as electrostatics is driving the separation, CDI is not significantly selective (Yoon et al., 2019). Performance of CDI can be improved by adding a membrane, which is referred to as membrane capacitive deionization (MCDI). Furthermore, CDI is a non-Faradaic process, i.e., there is no electron transfer between the electrode and the electrolyte. Conversely, pseudocapacitive and redox-active electrodes utilize surface-mediated Faradaic processes to increase ion uptake, separation efficiency, and selectivity (depending on the chemistry of the redox site) (Su and Hatton, 2016). In parallel, these systems can also be considered an aspect of "electrically switched ion exchange" (ESIX), which refers to a process enabling the selective removal of target ions from process or waste streams. In ESIX, the uptake and release of target ions are directly controlled by tuning the applied potential of an electroactive ion exchange film deposited onto a high-surface-area electrode (Rassat et al., 1999).

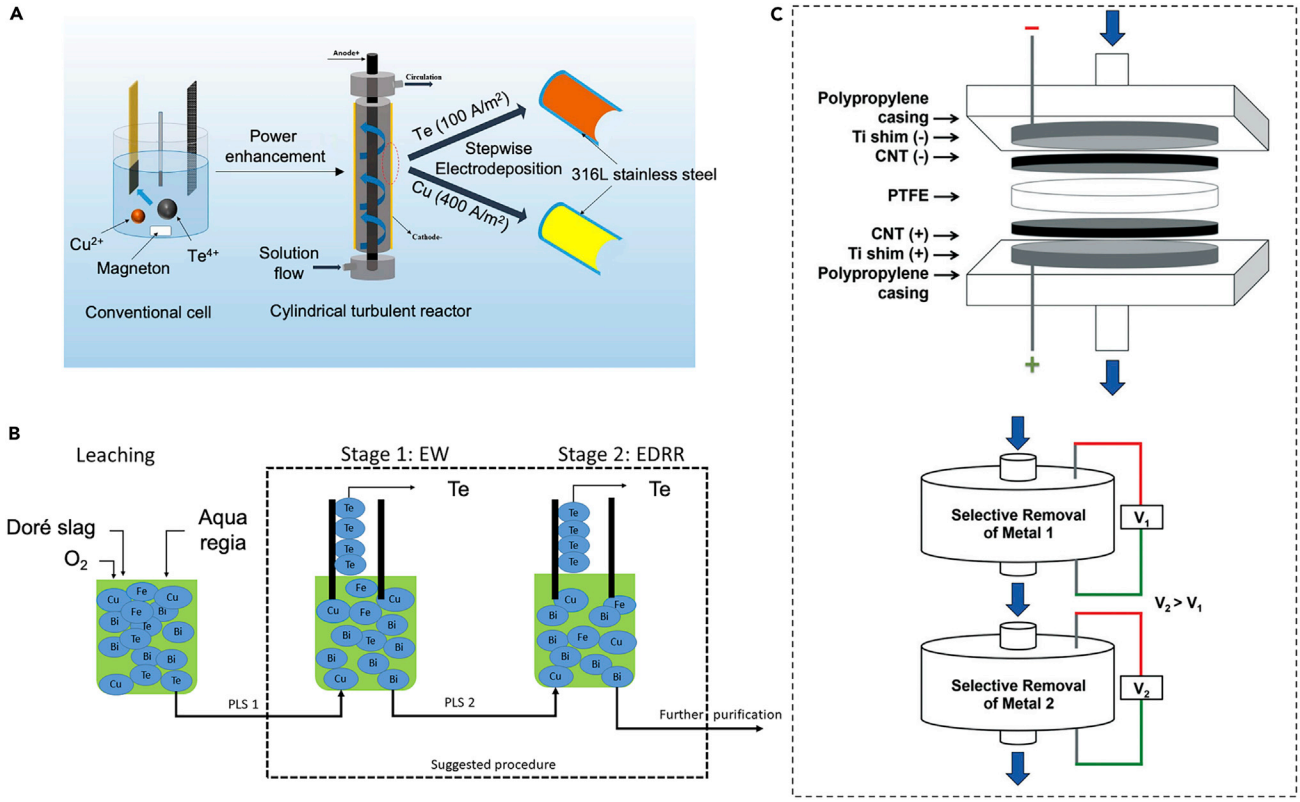

Figure 7. Selective electrodeposition of copper, tellurium, and rare earth elements

(A–C) (A) Schematic diagram of electroseparation of Cu and Te using a turbulent reactor. Reproduced with permission (Jin et al., 2018). Copyright 2018, American Chemical Society. (B) Schematic of tellurium recovery from a combined two-stage electrochemical process of electrowinning and electrodeposition-redox replacement. Reproduced with permission (Halli et al., 2019). Copyright 2019, Halli et al. (C) Schematic diagram of an electrodeposition system using carbon nanotube-based filters for the selective recovery of metals. Reproduced with permission (O'Connor et al., 2018). Copyright 2018, Royal Society of Chemistry, copyright 2018.

Porous capacitive electrodes

Hydration radius, ion valence, and applied voltage play key roles in the selectivity of CDI systems. When using activated carbon electrodes for electrosorption, divalent cations are removed more effectively than monovalent cations, whereas smaller ions are preferred over larger ions due to size affinity with the electrode pores. When the applied potential is increased, these separation trends are enhanced (divalent > monovalent cations, smaller > larger ions), so that selectivity is increased (Figure 8) (Hou and Huang, 2013; Li et al., 2016). As an example of valence difference selectivity, Cu^{2+} was preferentially removed over Na^{+} by CDI. Copper ions (Cu^{2+}, 50 mg L^{-1}) were selectively removed from a solution containing NaCl (0.001–0.1 mM), humic acid, and dissolved reactive silica by CDI (Huang et al., 2014).

Functionalization of the electrode's surface can further increase the selectivity of CDI systems. For instance, size-based selectivity of microporous carbon electrodes could be further enhanced by adding negatively charged carboxyl groups in the micropores through oxidation with nitric acid. The separation factor of K^{+} over Li^{+} increased from ~1 to 1.84 thanks to functionalization (Guyes et al., 2019). *Vanadium* was recovered using resin-activated carbon (RAC) composite electrodes. Selective capture of vanadium (V) (1,000 mg L^{-1}) over aluminum (3,000 mg L^{-1}), P (230 mg L^{-1}), and Si (35 mg L^{-1}) was achieved because Al, P, and Si are mainly adsorbed in the electric double layer, whereas vanadium (V) is adsorbed by the resins in the electrode. Impurities were then removed with diluted H_2SO_4, while V was recovered with a 10% NaOH solution (Bao et al., 2018). Another avenue for tuning selectivity is pore size distribution control. For example, small changes in the synthesis of hierarchical carbon aerogel monolith led to different ion selectivity; the monoliths were activated for 1 and 3 h, where activation refers to the preferential removal of the most reactive carbon atoms through a reaction with CO_2 at 950°C. For low activated cells (smaller mass loss during

Table 4. Separation of lithium: comparison between different electrochemical techniques based on separation performance metrics

Technique	Lithium concentration	Competing metals	Supporting electrolyte composition	Electrode/membrane material	Separation performance metric	Reference
Electrodeposition	0.05 g each of $LiFePO_4$, $LiMn_2O_4$, and $LiNi_{1/3}Co_{1/3}Mn_{1/3}O_2$		1 M $LiPF_6$ in ethylene carbonate-dimethyl carbonate	Lithium aluminum titanium phosphate (LATP) membrane	~99% pure Li metal or Li_2CO_3	(Bae et al., 2016)
Membrane capacitive deionization	1.8–14.5 mM Li^+	Mg^{2+} (1:1 Li^+:Mg^{2+})	Aqueous	Monovalent cation selective membrane	2.95 Li selectivity coefficient[a]	(Shi et al., 2019b)
Intercalation electrode membrane/ electrodialysis	1 M Li_2SO_4	0.1 M $CoSO_4$	0.1 M $NaSO_4$ (deintercalation compartment)	Mo_6S_8 and $LiMn_2O_4$ membranes	~100% selectivity rate[b]	(Guyot et al., 2012)
Intercalation electrode	276.5 mM Li^+	1,847 mM Na^+, 8.903 mM Ni^{2+}	Aqueous, 299 mg L^{-1} dissolved organic carbon	Lithium manganese oxide (λ-MnO_2)	>70 selectivity coefficient (per cycle)[c] 98.6 mol % purity[d]	(Kim et al., 2018c)
Intercalation electrode	0.035 mM Li^+	630 mM Na^+, 71 mM Mg^{2+}, 14 mM Ca^{2+} (desalination concentrate)	Aqueous	λ-MnO_2 and silver	>20 selectivity coefficient[e] 88% purity	(Joo et al., 2020)
Intercalation electrode	0.5, 5, 50 mM Li^+	~5 M NaCl (saturated)	Aqueous	$LiFePO_4$ and silver counter electrode	Final Li/Na ratio is 500 times the initial Li/Na ratio	(Pasta et al., 2012)
Intercalation electrode	234.8 mM Li^+	2,566.4 mM Na^+, 1,208.3 mM Mg^{2+}, 478.3 mM K^+, 5.7 mM Ca^{2+} (simulated brine, Salar de Uyuni, Bolivia)	Aqueous	Delithiated $LiNi_{1/3}Mn_{1/3}Co_{1/3}O_2$ cathode, silver anode	757 Li/Na, 398 Li/Mg, 468 Li/K, 14.7 Li/Ca separation factors[f] 96.4% purity[d]	(Lawagon et al., 2018)
Electrodialysis	150 mg L^{-1} Li^+	10–60 g L^{-1} Mg^{2+}	Aqueous	Anion and cation exchange membranes (Selemion CSO and ASA)	94.5% recovery rate 20.2–33.0 separation factor (or permselectivity)[g]	(Nie et al., 2017)
Electrodialysis/redox-flow battery analog	216 mM Li^+	3,306 mM Na^+, 473 mM K^+, 395 mM Mg^{2+}, 8 mM Ca^{2+} (simulated brine, Salar de Atacama, Chile)	Aqueous	Anion and cation exchange membranes, λ-MnO_2 as Li adsorbent, ferri-/ferrocyanide couple in the redox reaction channel	804 Li/Na, 387 Li/Mg selectivity coefficient[h]	(Kim et al., 2020c)

[a]Selectivity coefficient: ratio of the removal rate of Li over the removal rate of Mg.
[b]Selectivity rate: ratio $Li_t/(Li_t + Co_t)$, where Li_t and Co_t are the amount of lithium and cobalt transferred, respectively.
[c]Selectivity coefficient: ratio C_{Li}/C_{Na} between the concentration of lithium and sodium in the recovery reservoir. Li^+/Na^+ ratio in pristine water was 0.15.
[d]Purity(%):ratio of the concentrations $C_{Li}/(C_{Li} + C_{Na}) \times 100$.
[e]Selectivity coefficient: the molar amount of recovered Li^+ divided by the molar amount of cation M.
[f]Separation factor: $(C_{Li}/C_M)_f/(C_{Li}/C_M)_i$; ratio of Li over other metal M in the receiving solution, divided by the ratio of Li over M in the brine.
[g]Separation factor (or permselectivity): ratio of the transported ions (Li/Mg) over the Li/Mg ratio in the initial solution.
[h]Selectivity coefficient: e.g., in Li/Na, $(Li/M)_{adsorbed}/(Li/M)_{feed\ solution}$, corresponding to the ratio of the amount of adsorbed Li over Na, divided by the ratio of Li over Na in the feed solution.

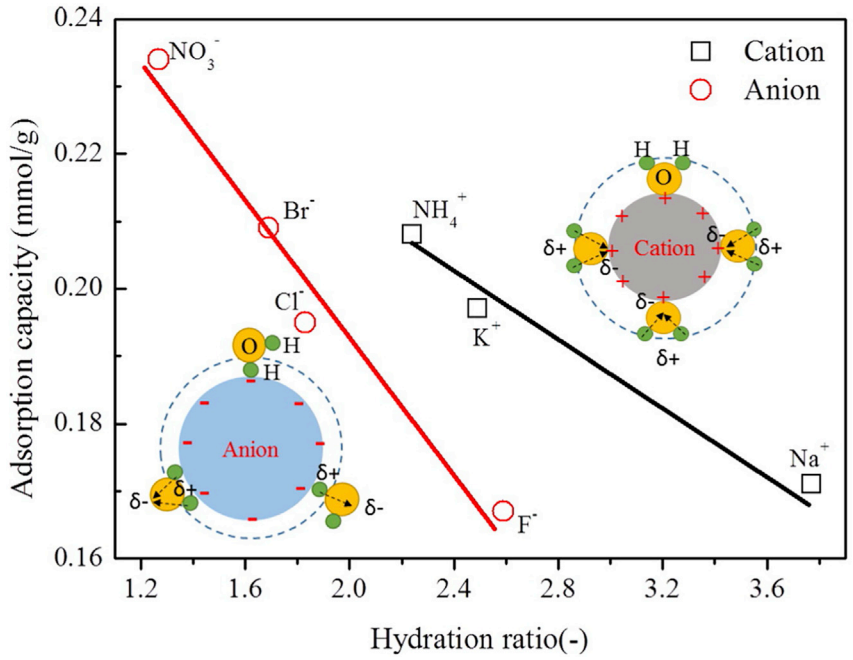

Figure 8. The dependence of adsorption capacity and selectivity on hydration ratio in a CDI-based electrosorption

Ions with smaller hydration ratio show high selectivity. Reproduced with permission (Li et al., 2016). Copyright 2016, Elsevier.

activation, and pore size distribution skewed toward smaller pores), Na^+ was removed, whereas no Ca^{2+} was adsorbed (selectivity coefficient >>1), whereas for the highly activated cells (higher mass loss during activation, and pore size distribution skewed toward bigger pores) Ca^{2+} was preferred over Na^+ (selectivity coefficient of 6.6 at 0.6 V, unexpectedly decreasing to 2.2 at 1.2 V) (Ceron et al., 2020).

Cobalt ions were removed by CDI employing an activated carbon cloth as electrode material, which resulted in 36.5% removal efficiency (with 5 mg L^{-1} initial cobalt concentration). Competitive removal in the presence of Sr and Cs showed poorer performance for the removal of cobalt (8.4%), with adsorption capacity for Co, Sr, Cs being 2.15, 2.19, and 1.84 mg g^{-1}, respectively (Liu et al., 2019b). Shi et al. separated lithium (Li^+) from magnesium (Mg^{2+}) by MCDI in aqueous solution (Shi et al., 2019b); lithium selectivity coefficient (defined as the ratio of the removal rate of lithium over the removal rate of magnesium) reached 2.95. Selectivity was achieved thanks to the monovalent selective cation exchange membrane, which would block the divalent Mg^{2+} cations. Chen et al. selectively removed *uranium* (VI) by CDI with an electrode made of boron phosphide nanosheets, reaching a maximum adsorption capacity of 2,584 mg g^{-1} (Chen and Tong, 2020). Selectivity of uranium (VI) over competing metal ions was achieved with excess factors from 100 to 10^4 of Sr^{2+}, Ba^{2+}, VO^{3-}, Cr^{3+}, Ca^{2+}, Co^{2+}, Cu^{2+}, Mn^{2+}, Mg^{2+}, Ni^{2+}, Fe^{3+}, Na^+, and K^+. The high selectivity of boron phosphide nanosheets for uranium (VI) was attributed to the strong coordination between phosphorus and uranium, and cyclic voltammetry showed no Faradaic reactions (Chen and Tong, 2020). In addition, Liu et al. employed amidoxime-functionalized electrode for selective uptake of uranium (Liu et al., 2017), promoting selective adsorption through a half-wave rectified alternating current. This approach enabled to solve conventional drawbacks from low concentration of uranium and the existence of other competing cations, by guiding the migration of target uranyl ions and also by avoiding the adsorption of unwanted species using an alternating current (Liu et al., 2017). *Palladium* was recovered by MCDI by using commercial cation and anion exchange membranes. Selectivity of Pd over ammonium ions was of 1.42–1.52, while removal efficiency was 99.07–99.94% (Kim et al., 2017a).

Intercalation electrodes

Transition metal ions or cations can be intercalated in lattice vacancies and interstitial sites of crystalline frameworks when a potential is applied. The intercalated ions are then released while discharging the

electrode. Intercalation electrodes capture ions and store them through a Faradaic process, rather than in the electrical double layer. This technique is also referred to as "battery desalination" and has been broadly explored for selective separations (e.g., critical elements, ammonium, phosphates) as well as for water desalination (Kim et al., 2017b; Son et al., 2020; Su and Hatton, 2016).

Various hexacyanoferrate materials were successfully employed as platforms for selective separations. Examples of intercalation electrodes include nickel hexacyanoferrate (NiHCF) (a Prussian blue [PB] analog), sodium manganese oxide, and iron or titanium phosphates. The transition metal ions incorporated in the host crystal structure are reduced upon application of an electric potential, so that cations are separated from solution and included in the pores of the crystal to maintain electroneutrality (Singh et al., 2018). Rassat et al. investigated nickel hexacyanoferrate (NiHCF) films for the selective and reversible removal of *potassium* and *cesium* ions from a stream containing sodium ions, using an ESIX process and reached separation factors of ~5 for K^+ over Na^+ and ~35 for Cs^+ over Na^+ (Rassat et al., 1999). The separation factor could be further improved for cesium. A NiHCF/porous three-dimensional carbon felt was used for the selective separation of Cs^+ through an ESIX process. Cs^+ was selectively adsorbed over Na^+, with a separation factor of 123 (Sun et al., 2012). NiHCF was also implemented for the separation of *platinum* (II) from nickel (II) (both at 1 ppm), using NiHCF nanoparticle-coated electrodes. A Pt uptake of ~160 mg g^{-1} at −0.6 V versus SCE was reached after 120 min, with negligible Ni uptake at the same potential. When removing Pt(II) in the presence of Co(II), both at 1 ppm, the performance of Pt(II) removal increases up to ~290 mg g^{-1} at −0.6 V versus SCE after 120 min, but simultaneous separation of Co^{2+} occurs up to ~60 mg g^{-1}. Pt(II) was in the anionic $PtCl_4^{2-}$ form, and the authors suggested a two-step separation mechanism, with chemisorption of Pt(II) on NiHCF followed by reduction to Pt(0) (Wang et al., 2020). Copper metal hexacyanoferrate nanoparticle films (CuHCF) were used as a platform for the selective removal of Co^{2+} (1 mg L^{-1}) from aqueous solution containing $LiNO_3$ (0.5–10.0 mg L^{-1}). The removal of Co^{2+} in solution with competing ions was studied; the presence of Li^+, Cu^{2+}, and Al^{3+} in solution did not affect the removal performance of Co^{2+}, whereas the presence of Ni^{2+} resulted in null Co^{2+} removal. Furthermore, in the case of Ni^{2+} it is not evident if this system was able to selectively remove Ni^{2+} from a Co^{2+}-Ni^{2+} solution, or if neither of the two metals was removed (Long et al., 2020). A Mo_6S_8 (Chevrel phase) electrochemical transfer junction (ETJ) was used for the separation of Co^{2+} from Ni^{2+}. The feed and recovery compartments of a membrane-type cell were separated by a Mo_6S_8 ETJ. Co^{2+} and Ni^{2+} were intercalated as $Co_xMo_6S_8$ and $Ni_xMo_6S_8$, with $0.5 \leq x \leq 2.0$. Upon application of potential only Co^{2+} ions crossed the ETJ so that almost complete separation (99%) was achieved for Co^{2+}. Selectivity was determined by the different ion fluxes through the Mo_6S_8 membrane (0.12 mmol h^{-1} cm^{-2} for Co^{2+} versus 1.5×10^{-3} mmol h^{-1} cm^{-2} for Ni^{2+}). Both the smaller peak split in cyclic voltammetry and lower impedance at constant potential demonstrated the facile insertion kinetics of Co^{2+} in Mo_6S_8 when compared with Ni^{2+}. The lower extraction potential for Co^{2+} in the recovery compartment cell and a more favorable interfacial ion-transfer kinetics were deemed responsible for the selectivity of Co^{2+} over Ni^{2+} (Guyot et al., 2013). Intercalation through two ETJs ($LiMn_2O_4$ and Mo_6S_8) was used for the simultaneous separation Li^+ and Co^{2+} from a solution containing both elements. Li^+ and Co^{2+} were selectively and continuously separated in two different cells when a potential was applied, with a 7-h transfer leading to 91% and 98% yields of lithium and cobalt, respectively. Selectivity rate was ~100%, with lithium ion fluxes across the ETJ in the 0.14–0.41 mmol h^{-1} cm^{-2} range (Guyot et al., 2012).

Secondary sources of lithium include spent batteries and desalination concentrate (the highly saline byproduct of water desalination). Intercalation has served as a promising platform for selective lithium recovery (Table 4). For example, lithium manganese oxide was used as a selective Li^+ recovering electrode in combination with an oxidant-generating electrode through an asymmetrical cell design (Kim et al., 2018c). Potential controlled capture/release of Li^+ over at least 5 cycles was achieved. This electrochemical setup was highly selective toward Li^+, reaching a purity of 98.6 mol % (Li^+ among cations) as well as simultaneously decomposing the organic pollutants when recovering Li^+ from spent batteries. The selectivity coefficient of Li^+ over Na^+ was >70 for every cycle; selectivity relies on the intercalation of Li^+ in spinel manganese oxide (λ-MnO_2), converting the electrode into $LiMn_2O_4$ (Kim et al., 2018c). High-purity lithium was selectively extracted from desalination concentrate in a pilot-scale system (Figure 9), reaching 88% purity with an enrichment factor of 1,800 (Li^+ concentration increasing from 0.035 to 62 mM). The electrodes, λ-MnO_2 and Ag, were converted to $Li_xMn_2O_4$ and $AgCl_x$ ($0 < x < 1$) when Li^+ was captured from the concentrate (Joo et al., 2020). The mechanism of Li^+ recovery through λ-MnO_2 was thoroughly investigated by Kim et al., finding that increasing the density of the electrode/electrolyte interface can increase lithium uptake

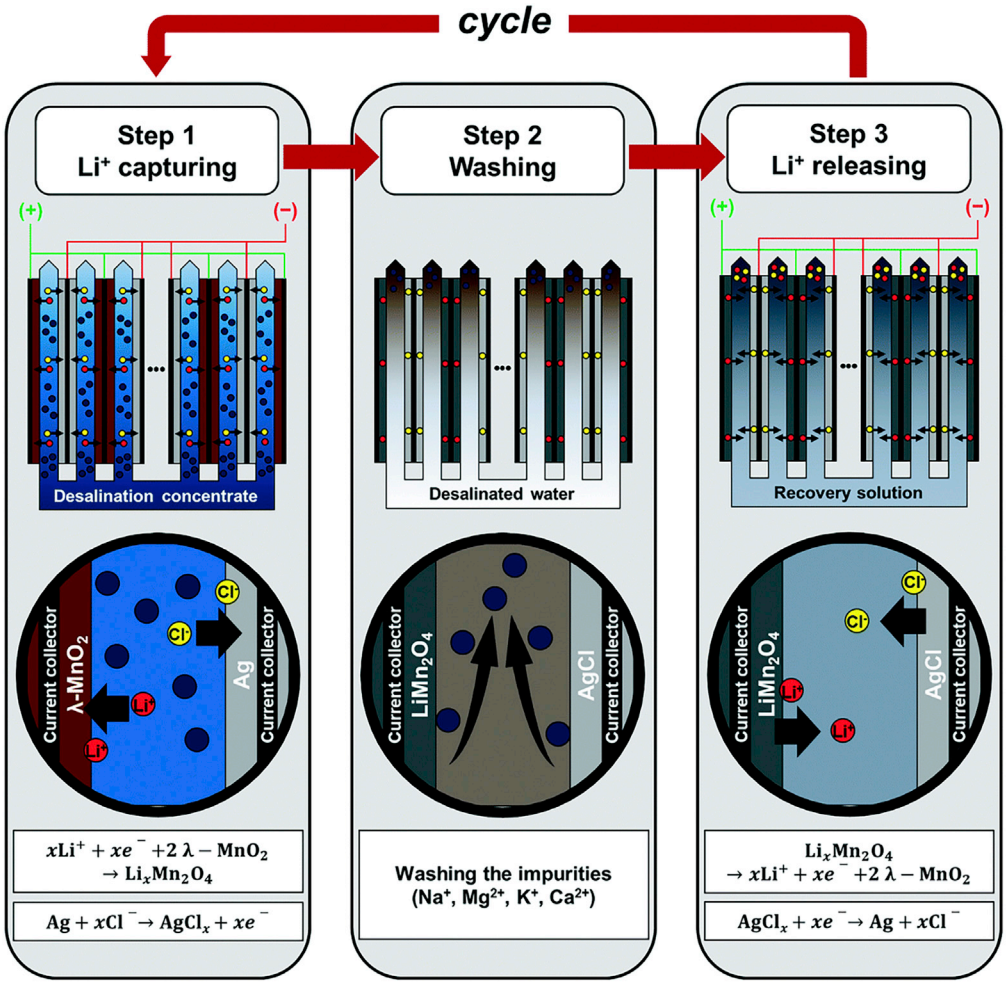

Figure 9. Schematic illustration of a three-step process for continuous recovery of lithium using λ-MnO_2/Ag electrode in a pilot-scale system

The three steps are Li^+ capture, washing, and Li^+ releasing. Reproduced with permission (Joo et al., 2020). Copyright 2020, Royal Society of Chemistry.

(Kim et al., 2020d). Lithium can also be selectively removed and up-concentrated using other intercalation cathode materials, such as $LiFePO_4$ coupled with a silver counter electrode. The $LiFePO_4$/Ag system could up-concentrate lithium to (Li^+: Na^+ = 5 : 1) when starting from a sodium-rich brine (Li^+: Na^+ = 1 : 100) (Pasta et al., 2012). Delithiated $LiNi_{1/3}Mn_{1/3}Co_{1/3}O_2$ (NCM) as cathode, with Ag as anode, could achieve Li^+ selective separation with potential controlled capture/release, yielding 96.4% pure Li^+ in optimal conditions and high separation factors after 20 cycles, i.e., Li^+ versus Na^+ (757), Mg^{2+} (398), K^+ (468), and Ca^{2+} (14.7) (Lawagon et al., 2018). A similar principle can be applied for the recovery of potassium, an important element for the production of fertilizers. Selective recovery of K^+ from seawater was achieved using Berlin-green intercalation electrodes (i.e., $Fe[Fe(CN)_6]$), with uptake of 117 μmol/g, 69.6% recovery of K^+, and separation factor of 141.7 for K^+ over Na^+. Selectivity depends on the different sizes of the hydrated ions of K^+ and Na^+, where only the smaller ion can penetrate the Berlin-green lattice (Shi et al., 2019c).

In some intercalation systems, there is not only selective removal of target elements (e.g., A over B), but it is also possible to switch the selectivity of the system (e.g., selectively removing B over A instead of A over B) just through potential tuning. For example, titanium disulfide (TiS_2)/carbon nanotubes electrodes could preferentially separate Cs^+ over Mg^{2+} for higher applied potentials (−219 to 26 mV versus Ag/AgCl, with molar selectivity ratio of 1.7 against Mg) while featuring an opposite selectivity (Mg^{2+} preferred over Cs^+) for lower applied potentials (−396 mV to −220 mV versu Ag/AgCl, molar selectivity of 31 against Cs^+) (Srimuk et al., 2018).

Redox-active electrodes

Redox-active interfaces, such as functionalized electrodes with electroactive polymers, have been shown to be an effective means for selective separations. These platforms have close connections to the above-present ESIX processes, i.e., capture/release of target ions is controlled through applied potential. Depending on redox-potential tuning, a low voltage can often be achieved for the electroswing process, thus preventing side reactions in water and resulting in higher energy efficiency. Redox-mediated separations are especially advantageous for metals with large reduction potentials (when compared with electrodeposition) and capture/release is triggered by potential control without need of added chemicals for regeneration of the adsorbents (Su, 2020b). Among other metallopolymers, poly(vinylferrocene) (PVFc) has been highly promising for selective separations of heavy metals oxyanions, where selectivity is attributed to the iron center of ferrocene and charge transfer. In particular, nanostructured pseudo-capacitive electrodes functionalized with ferrocene-based polymers showed selective and reversible separation of anionic *chromium, arsenic, molybdenum,* and *vanadium* oxyanions (Kim et al., 2020b; Su et al., 2018; Tan et al., 2020). The PVFc system featured 99% reversible working capacity, with an uptake of 100 mg (Cr) g^{-1} adsorbent (Su et al., 2018). This technique can work with a broad range of target metal concentrations (100 μg L^{-1}–500 mg L^{-1} $(NH)_4Cr_2O_7$ was investigated), removing the metals efficiently even in ultra-diluted conditions (i.e., 100 μg L^{-1} of chromium and arsenic) with 200-fold excess Cl^- (Su et al., 2018). Anionic arsenite was reversibly and selectively removed from competing anions such as Cl^- (arsenite: NaCl = 1 : 20) at a PVFc electrode with >90% efficiency, down to arsenite concentrations of 10 μg L^{-1} (Kim et al., 2020b). A hybrid electrochemical cell, comprising a PVFc functionalized anode and a nickel metal hexacyanoferrate (NiHCF) cathode, allowed to simultaneously separate cations and anions, in particular $Cr_2O_7^{2-}$, tetrahedral MoO_4^{2-}, and polymeric VO_3^-. The advantage of implementing a hexacyanoferrate cathode instead of an inert water-splitting cathode is that the energy requirement is reduced, higher separations are achieved, and pH increases are not encountered (Tan et al., 2020). An electrochemical flow cell was developed for the recovery of metal vanadium(V) oxyanions using an asymmetric cell design composed of PVFc-carbon nanotubes anode and a polypyrrole doped with anionic surfactant sodium dodecylbenzenesulfonate cathode (Figure 10). Selectivity tests were run, with a 20 mM $NaClO_4$ background electrolyte and 1 mM each of KVO_3, NaF, NaBr, $NaNO_3$, and Na_2SO_4 competing salts, resulting in a ~25-fold decrease in vanadium concentration, with insignificant adsorption of the other ions. Selectivity was >10 for vanadium over perchlorate (Hemmatifar et al., 2020).

Chen et al. conducted a systematic study on the selective separations of transition metal oxyanions through the modulation of structure or electrode potential using two redox-active polymers (Figure 11) (Chen et al., 2021). PVFc, which has a pendent ferrocene unit, and polyferrocenylsilane (PFS), which instead has the ferrocene unit in the main chain, showed different selectivity trends during multicomponent separation experiments of transition metals. Separation factors as high as 39 were reported (e.g., for vanadium over chromium oxyanions). Separation using real secondary effluent wastewater was also demonstrated. The mechanisms underlying selectivity were investigated using quantum mechanical calculations. Potential-dependent selectivity was found in the case of molybdenum versus chromium oxyanions; chromium was preferentially adsorbed with respect to molybdenum for lower applied potentials (0.5 V versus Ag/AgCl), whereas at higher applied potentials (1.0 V versus Ag/AgCl), more molybdenum was adsorbed relatively to chromium both for PVFc and PFS. Another example of swapping ion preference, based purely on potential, was the rhenium and molybdenum oxyanion couple. Notably, the release of adsorbed ions took place only through electrochemical control with no need of added regenerants (Chen et al., 2021).

Ion imprinting can also be used to achieve selectivity in electrochemical separations. Nickel ions could be selectively removed through Ni^{2+} ion-imprinted ferricyanide-embedded conductive polypyrrole (Ni^{2+}-FCN/PPy) films, with reversible uptake/release, achieving separation factors of 6.3 (Ni^{2+} over Ca^{2+}), 5.6 (Ni^{2+} over K^+), and 6.2 (Ni^{2+} over Na^{2+}) (Du et al., 2014). Ion imprinting was also used for developing electrodes selective to yttrium ions (Y^{3+}); removal of yttrium ions was achieved using Y^{3+} ion-imprinted ferricyanide-embedded polypyrrole film in a 0.1 M Y^{3+} solution. The removal mechanism was examined through electrochemical quartz crystal microbalance characterization, showing that the Y^{3+} imprinting is key for selectivity (Du et al., 2015). Selective recovery of silver (Ag^+) from a simulated wastewater containing simultaneously Ag^+, Zn^{2+}, Ni^{2+}, and Cu^{2+} (10 ppm of each) was possible through a polypyrrole film coupled with 2, 2′-dithiosalicylic acid. Carboxyl and disulfide bonds determined the selectivity toward silver of the electrode, and regeneration rates in the 80%–90% range up to 10 cycles (Niu et al., 2020).

Recently, redox-active metal organic frameworks (MOF) have also been shown to enable selective electrosorption. Selective recovery of Li^+ was obtained with an electroactive polypyrrole (PPy)-threaded HKUST-1

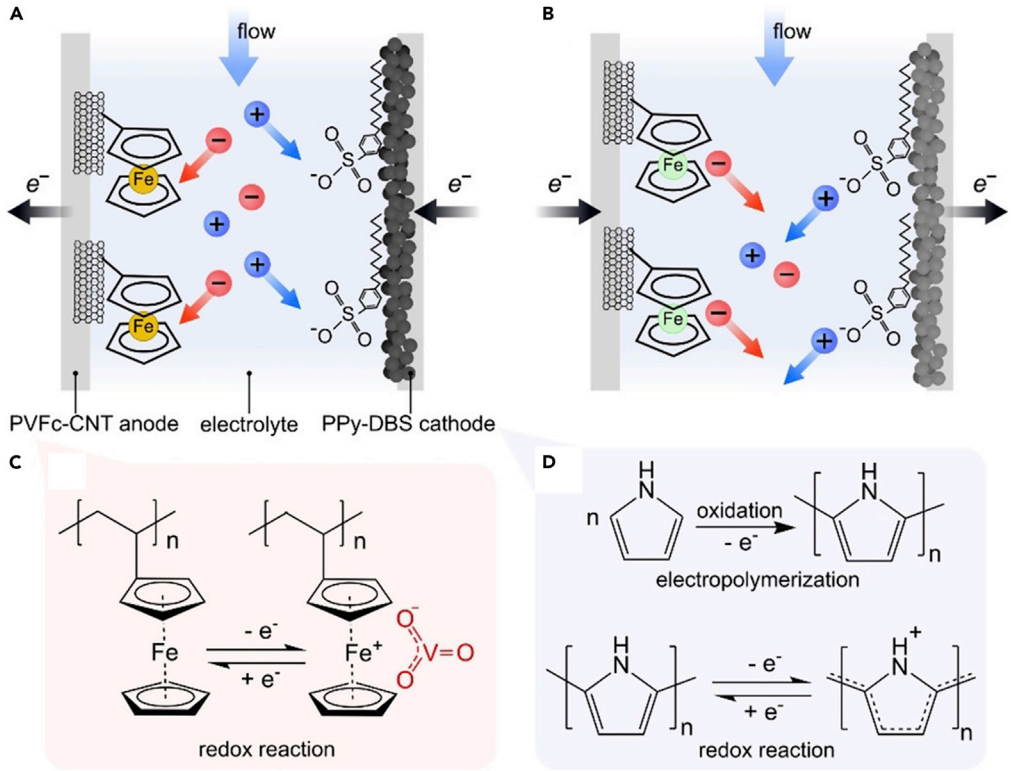

Figure 10. An asymmetric redox system for electrochemical recovery of vanadium oxyanions

(A–D) Schematic illustration of an asymmetric flow cell system employing PVFc-CNT anode and PPy-DBS cathode for reversible (A) capture and (B) release of anionic and cationic species. (C) Mechanism of capture/release by redox reaction of PVFc and (D) redox reaction of PPy. Reproduced with permission (Hemmatifar et al., 2020). Copyright 2020, Wiley-VCH Verlag GmbH & Co. KGaA, Weinheim.

MOF composite film, showing 37.55 mg g^{-1} adsorption capacity. The aqueous solution simultaneously contained 5 mg L^{-1} of Li^+, K^+, Na^+, Mg^{2+}, and Cu^{2+} (Wang et al., 2019a). When a reducing potential of −0.3 V versus SCE was applied, Li^+ ions could be selectively captured because the MOF size matched the Li^+ size. Selectivity coefficients of Li^+/K^+, Li^+/Na^+, Li^+/Mg^{2+}, and Li^+/Cu^{2+} (defined as the ratio of the distribution coefficients) reached 35.85, 119.14, 170.4, and 29.68 (Wang et al., 2019a).

Electrodialysis

Electrodialysis employs (1) an ion exchange or a bipolar ion exchange membrane and (2) an electrochemical potential as a driving force to separate ions (Figure 5C). Two important types of membranes that are used for electrodialysis include ion exchange membranes for conventional electrodialysis and bipolar membranes (Strathmann, 2010). Conventional electrodialysis utilizes ion exchange membranes with cation exchange capability containing negatively charged groups (e.g., sulfonate, carboxylate) or anion exchange capability containing positively charge groups (quaternary and tertiary amine) (Strathmann, 2010). In general, the permselectivity in electrodialysis-based process is largely affected by various factors, such as membrane design, solution concentration, electrochemical condition, etc. For example, it has been reported that there is a compromise between ionic conductivity and permselectivity in membrane design (Fan and Yip, 2019). Cross-linking also can increase selectivity and can decrease membrane swelling (Strathmann, 2010). Many of the processes that use electrodialysis also include pre- and post-treatments depending on the material being recovered. Many electrodialysis systems in this review are hybrid systems or include new membranes that improve the recovery of critical elements.

A possible electrodialysis technique for separating cobalt from nickel is the use of a hybrid process involving a liquid membrane made of trialkylbenzylammonium chloride and tri-n-octylamine in 1,2-dichloroethane to separate cobalt (II) chlorocomplexes from hydrochloric acid solutions (Sadyrbaeva, 2015). This

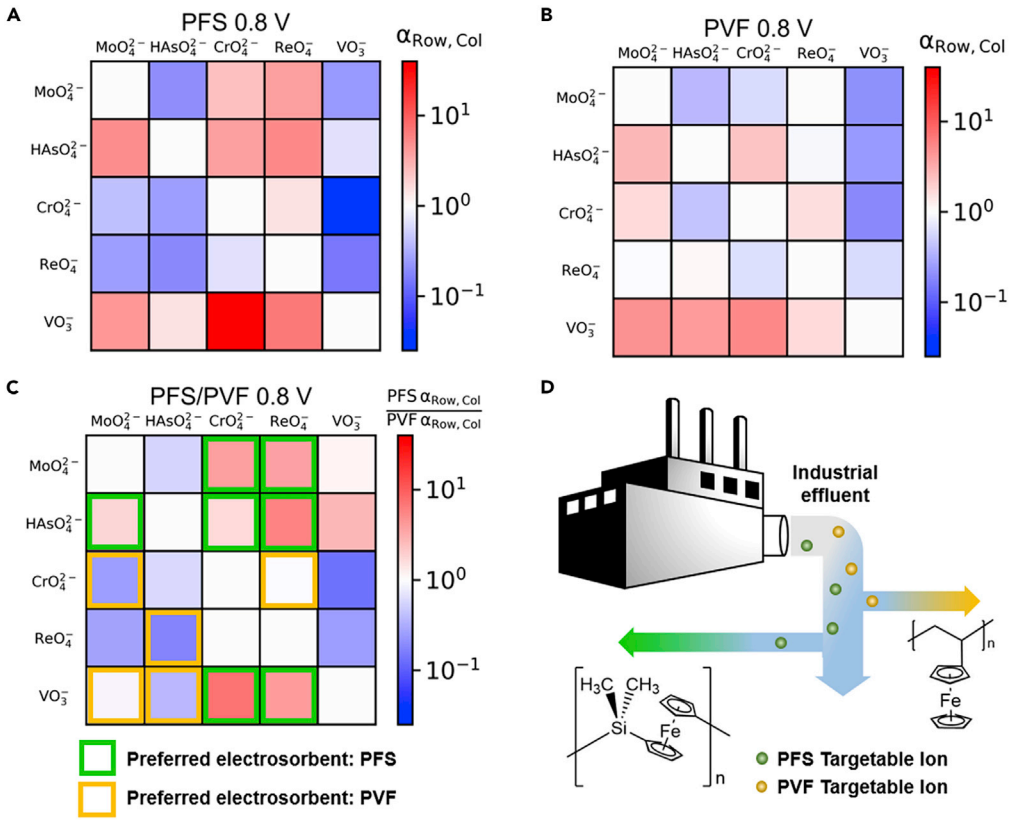

Figure 11. Structure-dependent selectivity of redox-metallopolymers for multicomponent metal separations

(A–D) Separation factors for binary separations of metal oxyanions using the redox-active metallopolymers (A) PFS and (B) PVFc. (C) PFS over PVFc selectivity factor ratios, highlighting which polymer adsorbs more and (D) schematic of the implementation of PFS and PVFc in a metal recovery process. Reproduced with permission (Chen et al., 2021). Copyright 2021, Wiley-VCH GmbH.

method works by combining electrodialysis with carrier-mediated transport where the liquid membrane provides greater selectivity and permeability compared with the traditional, solid electrodialysis membranes. As the current density and hydrochloric acid and cobalt (II) concentrations increased, the separation of cobalt (II) improved. From an equal concentration of cobalt and nickel, the separation factor for cobalt (II) was 145 with a separation factor of 330 for (10:1 = Ni:Co), and a separation factor of 400 for (1:10 = Ni:Co). Liquid membrane electrodialysis has also been used to separate rhenium, another critical element (Sadyrbaeva, 2015).

Selective separation of the radionuclides cobalt and cesium from a feed of dissolved lithium, cobalt, cesium, and boric acid was achieved using shock electrodialysis, i.e., the propagation of a shock wave creates a depletion zone, so that the system is divided into a region that is concentrated and a region that is deionized (Alkhadra et al., 2020). There was a compromise with this process between cobalt removed and water recovered. For example, the process removed 99.5% of the cobalt in the solution and recovered 43% of the water. To recover more water, the process could remove 98.5% of the cobalt while recovering 66% of the water (Alkhadra et al., 2020). Electrodialysis with bipolar membranes has been used to remove both chromium (VI) and chromium (III) from contaminated soil samples (Liu et al., 2020). The process used multiple feed streams alternating with separation compartments to decrease the energy consumption of the system. The simultaneous removal of chromium ions and the tunability of the process enabled high removal efficiencies of 99.8%. The recoveries of chromium (III) and chromium (VI) were 87% and 90%, respectively. Current density was the most important factor affecting the separation process (Liu et al., 2020).

A hybrid process using deep eutectic solvents and electrodialysis has been used as a proof of concept to separate *tungsten* and *arsenic* (Almeida et al., 2020). Deep eutectic solvents have been shown to be

advantageous in terms of cost, toxicity, and biodegradability when compared with other methods, so combining them with electrodialysis gives a more environment-friendly alternative to current techniques of recovery for both elements. The deep eutectic solvents used were choline chloride, malonic acid, oxalic acid, propionic acid, urea, and DL-lactic acid. The extraction efficiency turned out to be dependent on the deep eutectic solvent used. For example, choline chloride-based solvent exhibited typically higher extraction yields, with the mixture of choline chloride and malonic acid being more selective for arsenic and the mixture of choline chloride and oxalic acid more selective toward tungsten (Almeida et al., 2020).

Cerium tends to appear in the wastewater from ceric ammonium nitrate manufacturing. A hybrid method of using electrodialysis and vacuum membrane distillation was performed for the separation of cerium from nitrate (Ren et al., 2018). In nitric acid bath, cerium ion exists in the form of an individual cerium ion (Ce^{4+}) or it forms $Ce(NO_3)_n^{(4-n)+}$ complexes, both of which can be rejected by typical anion exchange membrane owing to charge or large molecular diameter, respectively. Increase in flow rate, current density, and nitric acid concentration all improved the removal of nitrate from the waste stream to the anodic compartment. The vacuum membrane distillation process concentrated the cerium solution and yielded a 99.9% rejection rate of cerium (Table 5) (Ren et al., 2018).

Electrodialysis was also used to reduce Mg/Li ratio of saline water with an originally high Mg content (Nie et al., 2017). A monovalent selective cation exchange membrane was fundamental for efficient separations (Figure 12A), with the Mg/Li ratio at optimal condition being reduced to 8.0 from an original ratio of 150 in the feed. A similar experiment was devised that involved potassium, sodium, and calcium as competing ions, and this resulted in Mg/Li ratios of 12.9, 9.9, and 9.8, respectively. Lower temperature, higher flow rate, and higher current density helped increase the separation of lithium from magnesium (Nie et al., 2017).

Kim et al. proposed the combined use of a lithium-selective chemical adsorbent, ion-exchange membranes, and homogeneous reversible redox reactions, in order to achieve selective lithium recovery in tandem with continuous enrichment of lithium (Figure 12B) (Kim et al., 2020c). The reversible redox couple ferri-/ferrocyanide in the outermost chamber was separated from the feed and ion-concentrated channel by anion exchange membranes, whereas the continuous redox reactions at the anode and cathode allowed for uninterrupted enrichment of the source water. At the same time, lithium-selective λ-MnO_2 enabled to recover the enriched lithium simultaneously, achieving high enrichment up to 37 mM starting from 5 mM Li^+ and 5 mM Na^+ and up to 0.6 mM starting from an extremely limited content of Li^+ (0.1 mM Li^+:9.9 mM Na^+), along with the highest selectivity coefficient of 804 for Li/Na and 387 for Li/Mg. This process showed significant selectivity toward lithium and successful up-concentration of the critical metal (Kim et al., 2020c).

Owing to its low concentration (usually below 15 ppm), electrodialysis is ideal for extracting *scandium* from secondary sources (Li et al., 2021). The operating parameters of applied current, feed concentration, and acidity were examined in relation to the recovery of scandium through electrodialysis. In particular, the authors investigated the selectivity of Sc^{3+} recovery in the presence of Al and Fe impurities to simulate a condition close to the red mud/bauxite residue. Interestingly, solution pH played an important role of modulating selectivity of Sc^{3+} removal compared with Fe^{3+} and Al^{3+}; with an increase in solution pH, the selective separation of Sc^{3+} over Fe^{3+} and Al^{3+} was achieved. Owing to the similar ionic size and chemical behavior, the selectivity mechanism is a complicated process at this point. Also, the existence of REE metals and common mono- and divalent cations severely decreased the selectivity, indicating that the selectivity of the removal process should be improved with the development of selective ion exchange membranes (Li et al., 2021).

Sewage sludge ash contains large amounts of *phosphorus*, but it requires pretreatment before use and separation from the heavy metals present. Electrodialysis was used to separate the phosphorus from the heavy metals, whereas bioleaching was used to solubilize it beforehand. The acidity of the solution proved to be the most important factor for phosphorus recovery. Electrodialysis experiments were conducted with a gold-coated copper electrode and had a 24.6% recovery rate of phosphorus into the anode chamber. This number is low, and it is likely due to precipitation in the middle and cathode chambers due to the lack of a continuous pH control to keep the phosphorus in solution, but the method does show promise (Semerci et al., 2019).

Coal ash could be a viable source for the recovery of rare earth metals, because the concentration of rare earth metals is much higher in coal ash than in conventional coal. Anthracite coal ash was preferable

Table 5. Separation of rare earths (including Sc and Y): comparison between different electrochemical techniques based on separation performance metrics

Technique	Target element(s)	Composition	Supporting electrolyte composition	Electrode/ membrane material	Separation performance metric	Reference
Selective anodic dissolution	Nd, Dy, Pr	$Nd_2Fe_{14}B$ magnets (contains Dy and Pr too)	/	/	/	(Prakash et al., 2016)
Electrochemical leaching/electrodeposition/ chemical precipitation	Nd, Dy, Pr	Nd-Fe-B magnet	$(NH_4)_2SO_4$, Na_3Cit, H_2SO_4	The magnet is used as anode	99.4% purity	(Xu et al., 2020)
Electrochemical alloy formation with reactive magnesium	Dy	$DyCl_3$ and $GdCl_3$ (1:1 mixture, 62 mM)	Eutectic bath of LiCl-KCl at 773 K	Tungsten and magnesium cathodes	98.4% extraction efficiency of Dy	(Yang et al., 2014)
Electrodeposition w/ formation of oxide	Cu, As, Eu, Nd, Ga, and Sc	1 mM of each target metal/metalloid	Aqueous, 100 mM Na_2SO_4. Ga was prepared in 100 mM NaCl	Unaligned carbon nanotubes encapsulated in polyvinyl alcohol filters	86%–96% max recovery (except for As). Metals are recovered as oxides	(O'Connor et al., 2018)
Redox-active functional electrode	Y	0.1 M Y^{3+}	Aqueous	Y^{3+} ion imprinted ferricyanide-embedded polypyrrole film	/	(Du et al., 2015)
Electrodialysis/vacuum membrane distillation	Ce	0.2 mM Ce^{4+}	Nitric acid	Anion exchange membranes (ASV, QPPO, CJMA-3), vacuum membrane distillation (TJ [the PVDF hollow fiber membrane produced by Tianjin University of Technology], DH [the PVDF hollow fiber membrane produced by Dehong CO., Ltd., China])	90% recovery efficiency of nitric acid at 0.1 mM for 6 h using CJMA-3 anion exchange membranes, 99.9% of Ce^{4+} rejected and concentrated during vacuum distillation	(Ren et al., 2018)
Electrodialysis	Sc	20 ppm, 40 ppm, 80 ppm Sc^{3+}	0.1M sulfuric acid as catholyte and anolyte in rinse compartments	Anion exchange membrane (PC SA [the anion-exchange membrane obtained from PCCell with strongly alkaline with polyester reinforcement]), cation exchange membrane (PC SK the cation-exchange membrane procured from PCCell with strongly acidic with sulfonic acid functional groups]), both from PCell	99.52% of Sc^{3+} removed from 20 ppm solution at 3 V	(Li et al., 2021)
Electrodialysis	Nd, Dy, Tb	Anthracite coal ash leached with nitric acid	Nitric acid, 0.01 M $NaNO_3$	Cation exchange membrane (CR67, MKIII, blank, GE Water & Processing Technologies)	Tb: 90% extracted, 55% recovered Nd: 80% extracted, 74% recovered Dy: 74% extracted, 62% recovered All at 50 mA	(Couto et al., 2020)

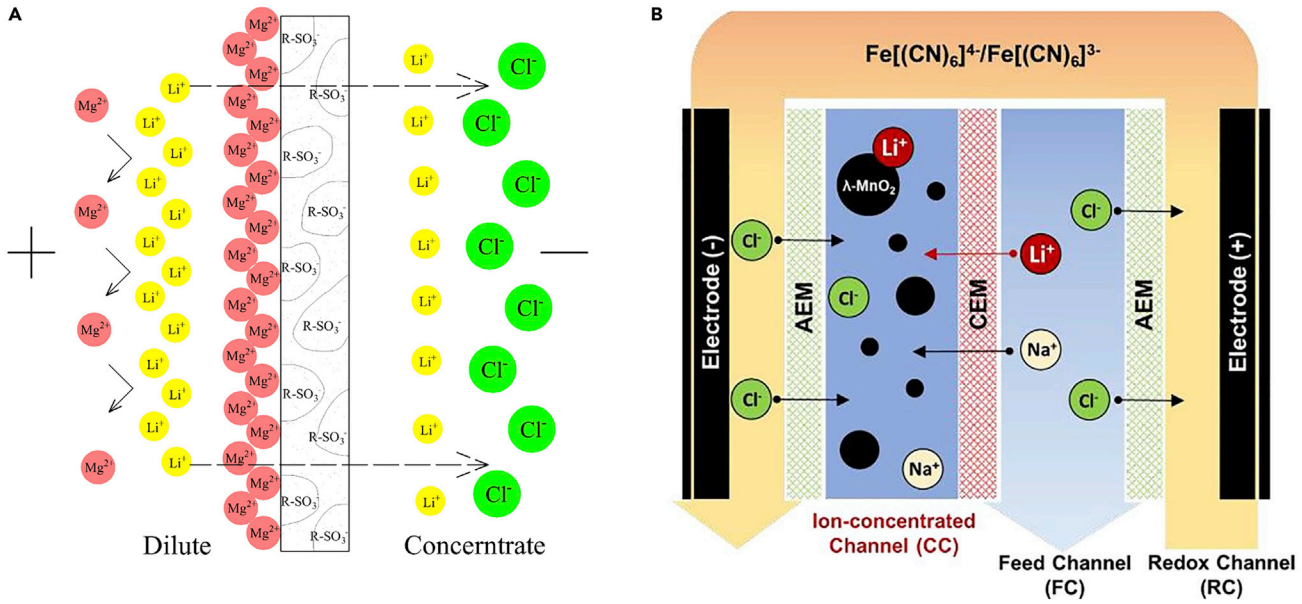

Figure 12. Electrochemical systems with ion-selective membranes for selective lithium recovery

(A) Schematic illustration of membrane-electrolyte interface. Reproduced with permission (Nie et al., 2017). Copyright 2017, Elsevier. (B) Schematic of redox-mediated system for the recovery of lithium, composed of redox channel, ion-concentrated channel, and feed channel. Reproduced with permission (Kim et al., 2020c). Copyright 2017, Elsevier.

because of its higher concentration of rare earth metals compared with bituminous coal ash (Couto et al., 2020). A process was developed that used three steps: solubilization, mobilization, and removal (Couto et al., 2020). The REEs of focus for the experiments were neodymium, dysprosium, and terbium; these elements were recovered from the fly ash by electrodialysis at 50 mA at 62%, 74%, and 55% recovery, respectively. The catholyte contained approximately 50% of the light REEs from the fly ash while also containing between 38% and 50% of the heavy rare earth metals (Table 5) (Couto et al., 2020). These experiments show that in a mixture of a wide range of REEs, electrodialysis was able to recover several of them satisfactorily. Despite advances in the field of metal recovery from ashes, further advances are needed to improve the selectivity and the efficiency of this process, as well as address the varying concentrations in ash composition depending on geographical location and waste content.

A recent approach, stemming from membrane-driven techniques, is to tune the selectivity by electrochemical stimulus and an associated redox-reaction. Li et al. developed an ion separation system based on an electrochemically tunable ion-sieve membrane (Li et al., 2020b). Here, the size of the sub-nanopores was modified by electrical control. The ion-sieve was made of Prussian blue, which can be electrochemically switched to Prussian white (PW), by applying a reducing potential for ~200 s. PW featured the same crystal structure of PB, but with a slightly larger crystal size. In the case of PW, small hydrated metal ions (Cs^+ and K^+) have a higher permeation rate than large hydrated ions (Li^+, Na^+, Mg^{2+}, and La^{3+}), whereas for PB permeation rate is lower for all ions (Figure 13) (Li et al., 2020b).

Electrocoagulation

In electrocoagulation, coagulants are generated *in situ* by oxidizing a sacrificial anode, which is usually composed of iron or aluminum. The oxidation process taking place at the anode continuously generates iron or aluminum cations and splits water into oxygen and H^+ cations, whereas water is split into hydrogen and OH^- anions at the cathode; metal ions and impurities might also be reduced at the cathode. Metal cations are immediately and spontaneously hydrolyzed to a variety of hydroxides and polymeric hydroxy complexes, depending on the pH of the electrolyte. These metallic hydroxides promptly bind to counter ions and dispersed particles, hence resulting in coagulation. The evolution of hydrogen and oxygen at the cathode and anode can help the physical separation of the flocculated pollutants via floatation (Figure 5D) (Mollah et al., 2004).

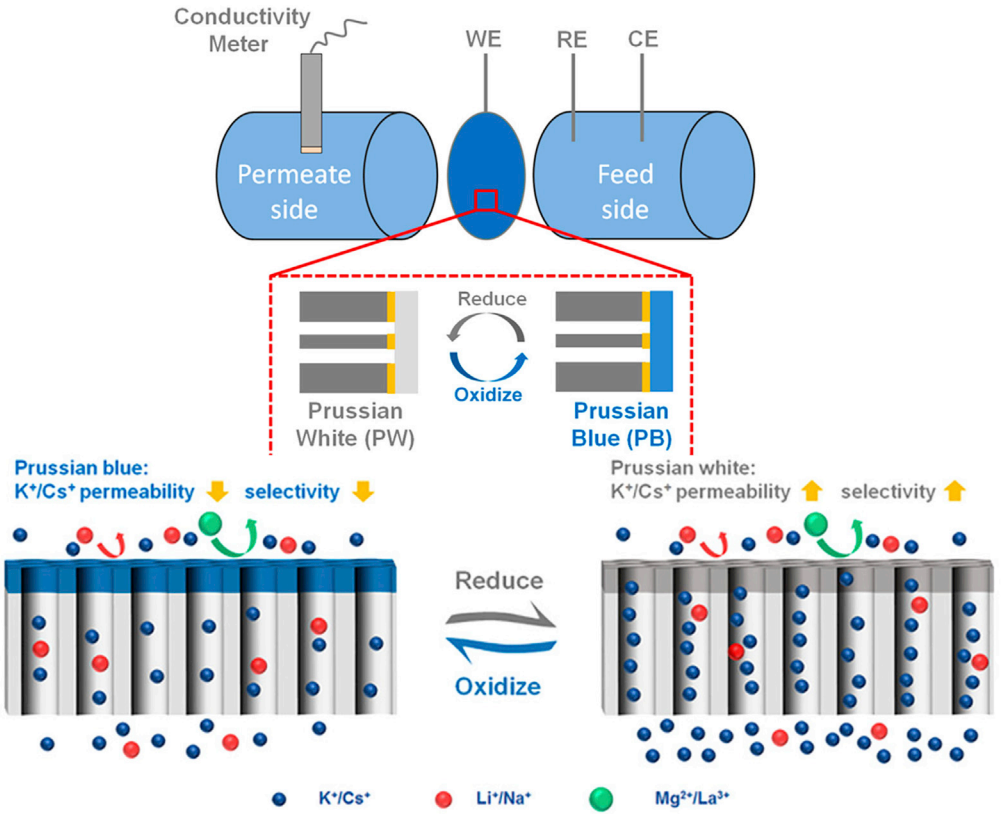

Figure 13. Schematic of the electrochemically tunable ion-sieve membrane based on Prussian blue coordination polymer for selective separations of cations

Reproduced with permission (Li et al., 2020b). Copyright 2020, American Chemical Society.

Despite advantages such as typically high removal efficiency, simple equipment, and easy operation, a serious limitation of EC is the lack of selectivity between multiple metals in solution (Mollah et al., 2004). For instance, copper, nickel, zinc, and manganese present in wastewater were removed simultaneously with a removal efficiency of 96% for Cu, Ni, and Zn, whereas Mn had a removal efficiency of 72.6% (Al Aji et al., 2012). Another key problem is the generation of sludge, which makes a further step of separation of the target metals from sludge necessary. Therefore, EC has been traditionally employed mainly for the purpose of ensuring high removal instead of delicate control of selectivity. For the recovery of critical elements, EC can be operated in a supporting electrolyte such as NaCl. For example, indium (III) was separated from synthetic wastewater by EC using an electrode pair of iron/aluminum (anode/cathode), where the removal efficiency reached 78.3% starting with an initial concentration of 20 mg L^{-1} indium (III) (Chou et al., 2009). Increasing the initial indium concentration reduced the removal efficiency (49.8% at 100 mg L^{-1} indium(III)). NaCl (50–200 mg L^{-1}) was added to increase the solution conductivity, thus obtaining a higher removal performance for higher NaCl concentrations with a lower energy consumption. Limitations of this technique include the presence of indium in a sludge with iron and other elements, and a high applied voltage required (10–30 V) (Chou et al., 2009). *Strontium* (25–100 mg L^{-1}) was removed by EC using stainless-steel anode and cathode, and aluminum anode and cathode, with NaCl (0.2–2 M) as supporting electrolyte. pH, current density, temperature, electrode material, initial strontium concentration, and the distance between the electrodes have a high impact on the removal efficiency, which reaches 93% in optimal conditions (Murthy and Parmar, 2011). Manganese (50–250 mg L^{-1}) was removed from model wastewater by EC using iron electrodes, achieving a maximum removal of 72.6%, with an energy consumption of ~49 kWh m^{-3}.

Electrochemical regeneration

Regeneration of the electrodes is essential for reuse of these costly materials, leading to a more feasible technology in the long term (Su and Hatton, 2017b). In conventional recovery processes, such as adsorption

and ion exchange, high chemical input (e.g., chelating agents, acids, or bases) is often required to regenerate spent adsorbent or ion exchange materials. On the other hand, one of the major advantages of electrochemically mediated processes is that regeneration of the materials can be done by modulating electrical input, offering ways to lower down the burden of the environmental and chemical footprint, and thus providing a competitive alternative to current industrial methods for critical element recovery (Strathmann, 2010; Su et al., 2016). However, only limited numbers of electrochemical recovery techniques address the regeneration stage, and in some cases, part of them are not still free from the use of chemical agents for regeneration.

The regeneration mechanisms of these processes can vary significantly depending on the electrochemical techniques used. Ideally, the regeneration step for electrodeposition involves anodic stripping to dissolve the separated metals in solid-phase to a liquid-phase regeneration electrolyte. The anodic regeneration of electrodeposited surfaces in critical metal recovery has not been extensively investigated, and in some cases, the regeneration of electrodeposited surfaces is known to be difficult for some critical elements (Chernyshova et al., 2020). For example, the anodic oxidation of electrodeposited cobalt and nickel was found to be irreversible according to cyclic voltammetry, in part due to the formation of insoluble oxides or hydroxide, resulting in much lower charge efficiency during anodic stripping when compared with the charge during cathodic deposition (Cojocaru et al., 2014; Grdeń and Jagiełło, 2012; Yu, 2017). It is worth noting that redox-promoted anodic stripping on polymer interfaces can enhance the regeneration efficiency. For example, the anodic stripping by redox-mediated oxidation has been shown to regenerate mercury-deposited polymer electrode (poly(3-hexylthiophene-2,5-diyl)-CNT [carbon nanotube] coated on titanium) with high reversibility (regeneration efficiency >85%) and fast regeneration kinetics (2.08×10^{-2} s^{-1} for P3HT-CNT/titanium, compared with 1.70×10^{-3} s^{-1} for bare titanium) for reversible mercury capture and release (Candeago et al., 2020), and similar approaches could be employed for other critical metals too.

Typically, the electrochemically-mediated regeneration in electrosorption-based techniques can be carried out without any chemical additives, or sometimes with the aid of acids or bases (Chernyshova et al., 2020). For example, the desorption process of three-dimensional graphene was achieved in two steps: first reversing polarity to detach adsorbed Na^+ ions, followed by acid treatment to desorb Pb^{2+} ions (Liu et al., 2017). For intercalation electrodes based on manganese oxides (birnessite), the regeneration mechanism has been observed via multi-cycles of redox reactions in Na_2SO_4. The regeneration efficiency was observed to decrease by 10% after the first cycle and then to 34% after the second cycle, possibly due to strong chemisorption of metal ions on birnessite surfaces (Yang et al., 2018). Another drawback of using manganese oxides is that Mn^{2+} ions can be released from the crystal structure, cause the decrease in specific capacitance of the material, and the structural degradation results in the irreversibility of adsorption (Peng et al., 2016).

Conductive and redox-active polymers have shown typically high reversibility and regenerability for ion capture, solely by electrical modulation and without the need of chemical regenerants (Weidlich et al., 2005). The polymer film will release cations when it is oxidized, or anions when it is reduced. As an example, conducting conjugated 2-2′-dithiodibenzoic acid (DTSA)/polyaniline (PANI) hybrid film achieved a regeneration rate of 99% after 30 cycles, controlled solely by switching electrode potentials (Wang et al., 2019b). One of the most promising redox-active systems, PVFc, works in a similar way and allows for easy regeneration, exhibiting 100% regeneration efficiency for heavy metal oxyanions (chromium and arsenic) (Kim et al., 2020b; Su et al., 2018). The reversible and electrochemically mediated capture and release based on electrosorption provides an environment-friendly and efficient way of up-concentrating selectively captured critical elements, adding industrial benefits, and creating possibilities for industrial process intensification (Su, 2020b).

The major purpose of the regeneration in electrodialysis processes is for clearing of fouling. Ideally, electrodialysis-based techniques can potentially have the advantage of not requiring a regeneration step or the addition of further chemicals (Barros et al., 2020). However, performance degradation due to fouling and scaling leads to ohmic resistance across the membrane and results in a serious impact on permselectivity over time. One approach is to reverse polarity for a certain duration to remove charged particles that have poisoned the membranes (Strathmann, 2010). However, in the case of some irreversible fouling, the system eventually needs to be cleaned with chemicals, or it needs to be replaced (Barros et al., 2020).

FUTURE PERSPECTIVES AND OPPORTUNITIES

As seen previously, recent developments in the electrochemical processes have realized controllable platforms for the selective recovery of critical elements, in combination with hydrometallurgical processes. Advances in the synthesis and fabrication of highly tailored selective interfaces, together with judicious electrochemical engineering, and desired cell architectures (e.g., highly efficient flow-through/turbulent cell configurations) can all contribute synergistically to sustainable metal recycling. Nevertheless, both fundamental and practical challenges still need to be resolved, before these systems can be deployed at a large scale. In this section, we discuss future directions and opportunities in electrochemical separation and hydrometallurgy processes that can point to pathways for future implementation.

Defining consistent selectivity metrics

There has often been a lack of a consistent framework in reporting selectivity metrics in electrochemical separations, which can hamper the development of new metal recycling technologies. For example, by inspection of Tables 3, 4, and 5, we can see that numerous metrics have been used (separation factor, selectivity factor, selectivity coefficient, selectivity rate), without a uniform approach; for instance, in the case of selective Li recovery, whereas some articles defined selectivity coefficient ($K_{Li/M}$) without accounting for feed solution concentration (Joo et al., 2020; Kim et al., 2018c), other studies defined the same term (selectivity coefficient) as the ratio of adsorbed Li to other metals divided by the ratio of amount of Li to other metal ions in the feed solution (Kim et al., 2020c). Here, we suggest implementing Equations 1, 2, and 3, which represent different aspects of the separation factor, as metrics for molecular selectivity of our electrode. The classic definition separation factor of species A over B contains information about the quantity separated (numerator) and also the quantity in the mainstream phase (denominator), as follows (Sandell, 1968; Seader et al., 1998):

$$\alpha_{A,B} = \frac{N_{A,\,ads}/N_{B,\,ads}}{N_{A,\,0}/N_{B,\,0}} \qquad \text{(Equation 1)}$$

where $N_{X,\,ads}$ is the number of moles of species X that were separated and $N_{X,0}$ is the initial quantity of X. The definition of separation factor can also include equilibrium concentration in solution (after separation) as follows (Chen et al., 2021; King, 2000; Srimuk et al., 2020):

$$\alpha_{A,B} = \left(\frac{N_{A,\,ads}/N_{B,\,ads}}{N_{A,\,sol}/N_{B,\,sol}}\right)_{eq} \qquad \text{(Equation 2)}$$

where $N_{X,\,ads}$ is the number of moles of X adsorbed at equilibrium and $N_{X,\,sol}$ is the number of moles of X remaining in solution after equilibrium has been reached. Note that Equation 2 does not consider the ratio at initial conditions, but after reaching equilibrium (Srimuk et al., 2020). The advantage of such definition is that the separation factor can be interpreted as the equilibrium constant of the adsorption reaction A + B-S = A-S + B, where X-S indicates that the molecule X is adsorbed to the site S, i.e., $K_{eq} = \frac{[A-S][B]}{[A][B-S]}$ (Chen et al., 2020). Separation factors defined as in Equation 2 can bring insight into the equilibrium behavior of the separation system used. In both Equations 1 and 2, selectivity for A with respect to B corresponds to $\alpha_{A,B}>1$, whereas selectivity for B over A implies $\alpha_{A,B}<1$ (Chen et al., 2021; Srimuk et al., 2020). In the case of flow systems with a feed and a stripping solution, the separation factor can be defined as:

$$\alpha_{A,B} = \frac{N_{A,\,strip\,sol}/N_{B,\,strip\,sol}}{N_{A,\,feed\,sol}/N_{B,\,feed\,sol}} \qquad \text{(Equation 3)}$$

where $N_{X,\,strip\,sol}$ is the number of moles of species X in the stripping solution and $N_{X,\,feed\,sol}$ is the number of moles of species X in the feed solution at initial conditions. When multiple species are present, adaptations of Equations 1, 2, and 3 may be needed, and it is necessary to specify all the possible separation factors α_{T_i,C_j} where T_i are the target species and C_j are the competing species (Lawagon et al., 2018). Furthermore, we advise the approach suggested by Battistel et al. for lithium for all the other critical elements, ideally agreeing also on standard target and competing elements concentrations, as well as background electrolyte concentrations (Battistel et al., 2020).

Speciation control

Considering chemical transformations within the liquid medium is critical for hydrometallurgical processes, especially complex aqueous or organic speciation of various metals. The dilute concentration of metals in waste streams makes it difficult to capture target ions selectively and efficiently. In this regard, speciation

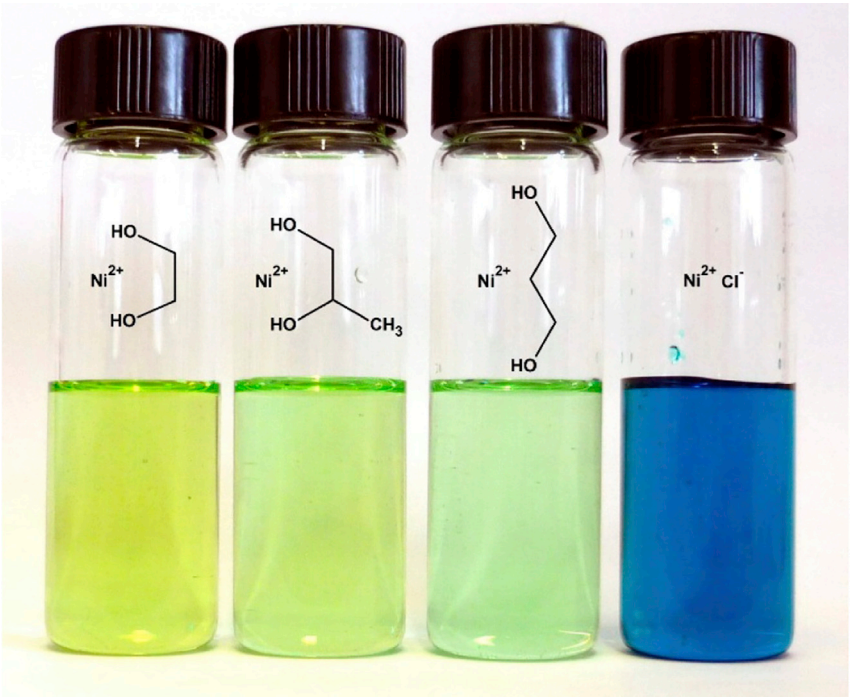

Figure 14. Speciation control of nickel in deep eutectic solvents

Control of the speciation of nickel: solutions of 100 mM $NiCl_2 \cdot 6H_2O$ in deep eutectic solvents using 1,2-ethanediol, 1,2-propanediol, and 1,3-propanediol as hydrogen-bonding donors, and in [C6mim][Cl]. Reproduced with permission (Hartley et al., 2014). Copyright 2014, American Chemical Society.

control can be leveraged for the effective separation and recovery from liquid streams; providing distinct chemical properties given by control of speciation offers a path for discrimination between metals with similar properties (Lee and Oh, 2005). Some ligands, such as cyanide and thiosulfate, bind strongly to metals and alter the electrochemical behavior of metals; their reduction potentials are controlled depending on their speciation and electrolytic condition (e.g., concentration of ligand, pH). For example, thermodynamic analysis has been carried out to identify potential levels where selective deposition of dilute concentrations of silver or gold from concentrated copper-containing solutions occurs—the potentials turned out to be shifted to cathodic direction as the concentration of thiosulfate increased (Alonso et al., 2007; Reyes Cruz et al., 2002; Spitzer and Bertazzoli, 2004), providing a way of modulating selectivity via speciation and potential control. In addition, some weakly binding ligands can exhibit the same speciation effect by having high concentration; for example, concentrated chloride leads to different electrodeposition behavior of Cu and Te, enabling the selective extraction of the different metals (Jin et al., 2018). These ligands, either strong or weak, indeed have been employed as lixiviants in conventional hydrometallurgical processes—therefore, the electrochemical recovery process can take benefits from former leaching processes in relation to the speciation chemistry, and the judicious selection of appropriate lixiviants and electrochemical methods allows for a continuous, integrated approach for selective separations. Previous speciation control has been, in most cases, focused on electrodeposition processes, but we believe this can be also adopted with different electrochemical methods, such as electrosorption by targeting charge-transfer and specific interaction between redox groups and ligands. The conventional complexing agents have issues related to safety and environmental impact, whereas we expect that ionic liquids or deep eutectic solvents can be green alternatives to toxic ligands for the control of speciation. For example, Hartley et al. revealed that the reactivity and speciation of metals depends on the type of deep eutectic solvents and ionic liquids (Hartley et al., 2014); nickel speciation was relatively more susceptible to water compared with other metals, and also it exhibited a very unusual coordination in diol-based deep eutectic solvent (Figure 14). In this way, the ion-rich nature of ionic liquids or deep eutectic solvents can be used for the control of speciation and for providing distinct chemical properties for target metals. It is worth noting that ionic liquids and deep eutectic solvents can also be used for the leaching/digesting of metal ores or electronic wastes (Abbott et al., 2011; Tran et al., 2019), enabling the integrated approach of

electrochemically assisted ionometallurgy. Some properties of ionic liquids/deep eutectic solvents, such as wide electrochemical window and low volatility, make them the desirable media for electrochemical recovery processes. At the same time, other properties, for example, the tunability of physicochemical characteristics and no need of high temperatures, allow for greener and milder methods for processing in urban mining. The judicious design of next-generation lixiviant/electrolytes can play an important role for target-specific separation in hydrometallurgical processes. In addition, combininginterfacial control (*e.g.*, redox-active adsorbent) with electrolyte engineering is expected to provide new opportunities for developing selective separations.

The speciation of recovered elements is also very important as it determines the necessity of further processing for secondary use. The main advantage of the electrochemical pathways is the possible recovery of metals in preferred speciation forms. For example, in many electrodeposition cases, final products are recovered as zero-valent metallic species (Jin et al., 2018; Jin and Zhang, 2020; Maguyon et al., 2012; Padhy et al., 2016; Yang et al., 2014; You et al., 2012). In other cases, metals with negative reduction potential can be recovered as air-stable precursors; for example, lithium can be recovered in the form of air-stable Li_2CO_3 or LiOH (Bae et al., 2016; Hoshino, 2015). This flexibility in speciation control highlights the modularity of electrochemical technologies, which even enables the design of reactions in opposite electrode chambers in a way that brings about intended speciation (Bae et al., 2016).

Combined interface and electrochemical engineering for process intensification

Recent advances in the synthesis of highly tailored redox interfaces offer a promising platform for the future development of electrochemical hydrometallurgy, especially for metals that have largely negative reduction potential and thus are not easily electrodeposited. However, many studies reported so far feature selective metal recovery in synthetic binary mixtures. Even though the studies in simple mixtures enable quick evaluation of new recovery methods and provide important information, these results can often be limited when inferring performance under realistic conditions—multicomponent, complex mixtures with a broader range of simultaneous competing targets (Su, 2020a). In spite of recent advances in designing selective interfaces, detailed interactions of electrodes with complexing ligands or under ionic liquid/deep eutectic solvents is quite unknown. Thorough investigation of interfacial properties and redox process, especially in the presence of chelating agents or under nonaqueous environment, is necessary and can be assisted by *in situ* spectroscopic methods and/or computational calculations of molecular level interactions. For selective recovery of minority components under realistic conditions, the understanding of mechanisms such as electrostatics, charge transfer, and hydrophobic interaction is required for separation of metals with similar properties (e.g., reduction potential).

In parallel, judicious electrochemical engineering (e.g., the design of counter electrodes, types of electrical stimuli, optimizing electrochemical parameters) can significantly improve the separation and energy efficiency. Combined efforts for engineering of heterogeneous electrode interfaces, electrolytes, fluid dynamic behavior, and operational parameters are needed. For example, judicious selection of cell architecture and electrochemical design has enabled tandem separations on both working and counter electrodes (Su et al., 2017), as well integrated reactive separations (Kim et al., 2020a, 2020b; Su et al., 2018), with energy consumption being minimized through overpotential control. We believe that synergistic design of molecular interfaces and electrochemical engineering can pave the way to a promising future for process intensification.

In sum, the increasing demand and decreasing supply of global critical raw materials call for the development of the sustainable recovery and recycling of the valuable elements. Hydrometallurgical processes have been studied for various recycling applications, with increasing industrial-scale implementations in the last decades. There have been significant improvements in the leaching stage with greener lixiviants, as well as new approaches using supercritical CO_2 for sustainable extraction. However, at the same time, several issues with regard to chemical footprint, generation of wastes, slow leaching, and molecular selectivity still remain. In mitigating these challenges, electrochemical separations can be naturally coupled with existing hydrometallurgical processes. Electrochemically assisted methods can be integrated with renewable energy sources, minimize secondary pollution, and provide remarkable selectivity, thus improving the overall sustainability of the process. However, there are significant challenges to be circumvented at multiple scales, ranging from molecular design to electrochemical engineering. Ensuring acceptable recovery uptakes, separation factor, and rates at an industrial scale can significantly impact size and capital costs of

electrochemical systems. Rigorous studies in faradaic/current efficiency of electrochemical processes, life cycle, and technoeconomic analysis are thus required to facilitate the transition of laboratory-scale studies into industrial implementation. In sum, we believe that selective electrochemical technologies, in conjunction with green hydrometallurgical processes, can pave a path toward sustainable materials recycling and critical element recovery.

ACKNOWLEDGMENTS

The information, data, or work presented herein was funded in part by the Advanced Research Projects Agency-Energy (ARPA-E), U.S.Department of Energy, under Award Number DE-AR0001396. The work is also partly supported by US Department of Energy, Office of Basic Energy Sciences under Award Number DOE DE-SC0021409. Research on hydrometallurgical technologies by A.-H.A.P. introduced in this review includes the work supported by Korea Institute of Energy Technology Evaluation and Planning (KETEP) grant funded by the Korea government (MOTIE) (No. 20188550000580) and National Science Foundation (CBET 1706905).

AUTHOR CONTRIBUTIONS

Conceptual development: K.K. and X.S.; investigating and drafting the manuscript: K.K., R.C., G.R., and D.R.; revision and editing: K.K., R.C., G.R., D.R., A.-H.A.P., and X.S.; illustrating figures: K.K., R.C., G.R., and A.-H.A.P.; supervision: X.S.; all authors read and approved the final manuscript draft.

DECLARATION OF INTERESTS

The authors declare no competing interests.

REFERENCES

Abbott, A.P., Frisch, G., Hartley, J., and Ryder, K.S. (2011). Processing of metals and metal oxides using ionic liquids. Green. Chem. *13*, 471–481.

Ajiboye, A.E., Olasehinde, F.E., Adebayo, O.A., Ajayi, O.J., Ghosh, M.K., and Basu, S. (2019). Extraction of copper and zinc from waste printed circuit boards. Recycling *4*, 36.

Akcil, A., Erust, C., Gahan, C.S., Ozgun, M., Sahin, M., and Tuncuk, A. (2015). Precious metal recovery from waste printed circuit boards using cyanide and non-cyanide lixiviants – a review. Waste Manage *45*, 258–271.

Al Aji, B., Yavuz, Y., and Koparal, A.S. (2012). Electrocoagulation of heavy metals containing model wastewater using monopolar iron electrodes. Separation Purif. Technol. *86*, 248–254.

Alkhadra, M.A., Conforti, K.M., Gao, T., Tian, H., and Bazant, M.Z. (2020). Continuous separation of radionuclides from contaminated water by shock electrodialysis. Environ. Sci. Technol. *54*, 527–536.

Almeida, J., Craveiro, R., Faria, P., Silva, A.S., Mateus, E.P., Barreiros, S., Paiva, A., and Ribeiro, A.B. (2020). Electrodialytic removal of tungsten and arsenic from secondary mine resources — deep eutectic solvents enhancement. Sci. Total Environ. *710*, 136364.

Alonso, A.R., Lapidus, G.T., and González, I. (2007). A strategy to determine the potential interval for selective silver electrodeposition from ammoniacal thiosulfate solutions. Hydrometallurgy *85*, 144–153.

Altimari, P., Schiavi, P.G., Rubino, A., and Pagnanelli, F. (2019). Electrodeposition of cobalt nanoparticles: an analysis of the mechanisms behind the deviation from three-dimensional diffusion-control. J. Electroanal. Chem. *851*, 113413.

Ambaye, T.G., Vaccari, M., Castro, F.D., Prasad, S., and Rtimi, S. (2020). Emerging technologies for the recovery of rare earth elements (REEs) from the end-of-life electronic wastes: a review on progress, challenges, and perspectives. Environ. Sci. Pollut. Res. Int. *27*, 36052–36074.

Armstrong, R.D., Todd, M., Atkinson, J.W., and Scott, K. (1996). Selective electrodeposition of metals from simulated waste solutions. J. Appl. Electrochem. *26*, 379–384.

Armstrong, R.D., Todd, M., Atkinson, J.W., and Scott, K. (1997). Electroseparation of cobalt and nickel from a simulated wastewater. J. Appl. Electrochem. *27*, 965–969.

Bae, H., Hwang, S.M., Seo, I., and Kim, Y. (2016). Electrochemical lithium recycling system toward renewable and sustainable energy technologies. J. Electrochem. Soc. *163*, E199–E205.

Baldé, C.P., Forti, V., Gray, V., Kuehr, R., and Stegmann, P. (2017). The Global E-Waste Monitor (United Nations University (UNU), International Telecommunication Union (ITU) & International Solid Waste Association (ISWA)).

Banthia, S., Sengupta, S., Mallik, M., Das, S., and Das, K. (2017). Substrate effect on electrodeposited copper morphology and crystal shapes. Surf. Eng. *34*, 485–492.

Bao, S., Duan, J., and Zhang, Y. (2018). Recovery of V(V) from complex vanadium solution using capacitive deionization (CDI) with resin/carbon composite electrode. Chemosphere *208*, 14–20.

Barros, K.S., Martí-Calatayud, M.C., Pérez-Herranz, V., and Espinosa, D.C.R. (2020). A three-stage chemical cleaning of ion-exchange membranes used in the treatment by electrodialysis of wastewaters generated in brass electroplating industries. Desalination *492*, 114628.

Battistel, A., Palagonia, M.S., Brogioli, D., La Mantia, F., and Trocoli, R. (2020). Electrochemical methods for lithium recovery: a comprehensive and critical review. Adv. Mater. *32*, e1905440.

Behnamfard, A., Salarirad, M.M., and Veglio, F. (2013). Process development for recovery of copper and precious metals from waste printed circuit boards with emphasize on palladium and gold leaching and precipitation. Waste Manage *33*, 2354–2363.

Bennion, D.N., and Newman, J. (1972). Electrochemical removal of copper ions from very dilute solutions. J. Appl. Electrochem. *2*, 113–122.

Birloaga, I., De Michelis, I., Ferella, F., Buzatu, M., and Veglio, F. (2013). Study on the influence of various factors in the hydrometallurgical processing of waste printed circuit boards for copper and gold recovery. Waste Manage *33*, 935–941.

Calgaro, C.O., Schlemmer, D.F., Bassaco, M.M., Dotto, G.L., Tanabe, E.H., and Bertuol, D.A. (2017). Supercritical extraction of polymers from printed circuit boards using CO2 and ethanol. J. CO2 Utilization *22*, 307–316.

Calgaro, C.O., Schlemmer, D.F., da Silva, M.D.C.R., Maziero, E.V., Tanabe, E.H., and Bertuol, D.A. (2015). Fast copper extraction from printed circuit boards using supercritical carbon dioxide. Waste Manage *45*, 289–297.

Candeago, R., Kim, K., Vapnik, H., Cotty, S., Aubin, M., Berensmeier, S., Kushima, A., and Su,

X. (2020). Semiconducting polymer interfaces for electrochemically assisted mercury remediation. ACS Appl. Mater. Interfaces *12*, 49713–49722.

Ceron, M.R., Aydin, F., Hawks, S.A., Oyarzun, D.I., Loeb, C.K., Deinhart, A., Zhan, C., Pham, T.A., Stadermann, M., and Campbell, P.G. (2020). Cation selectivity in capacitive deionization: elucidating the role of pore size, electrode potential, and ion dehydration. ACS Appl. Mater. Interfaces *12*, 42644–42652.

Chen, L., and Tong, D.G. (2020). Amorphous boron phosphide nanosheets: a highly efficient capacitive deionization electrode for uranium separation from seawater with superior selectivity. Separation Purif. Technol. *250*, 117175.

Chen, R., Feng, J., Jeon, J., Sheehan, T., Rüttiger, C., Gallei, M., Shukla, D., and Su, X. (2021). Structure and potential-dependent selectivity in redox-metallopolymers: electrochemically-mediated multicomponent metal separations. Adv. Funct. Mater. *31*, 2009307.

Chen, R., Sheehan, T., Ng, J.L., Brucks, M., and Su, X. (2020). Capacitive deionization and electrosorption for heavy metal removal. Environ. Sci. Water Res. Technol. *6*, 258–282.

Chernyshova, I., Bakuska, D., and Ponnurangam, S. (2020). Selective recovery of critical and toxic elements from their low-concentrated solutions using surface-based electrochemical separation methods. In Multidisciplinary Advances in Efficient Separation Processes (American Chemical Society), pp. 115–165.

Chou, W.L., Wang, C.T., and Huang, K.Y. (2009). Effect of operating parameters on indium (III) ion removal by iron electrocoagulation and evaluation of specific energy consumption. J. Hazard Mater. *167*, 467–474.

Chyan, O., Arunagiri, T.N., and Ponnuswamy, T. (2003). Electrodeposition of copper thin film on Ruthenium. J. Electrochem. Soc. *150*, C347–C350.

Cojocaru, A., Mares, M.L., Prioteasa, P., Anicai, L., and Visan, T. (2014). Study of electrode processes and deposition of cobalt thin films from ionic liquid analogues based on choline chloride. J. Solid State Electrochem. *19*, 1001–1014.

Couto, N., Ferreira, A.R., Lopes, V., Peters, S.C., Mateus, E.P., Ribeiro, A.B., and Pamukcu, S. (2020). Electrodialytic recovery of rare earth elements from coal ashes. Electrochim. Acta *359*, 136934.

Cui, C.Q., Jiang, S.P., and Tseung, A.C.C. (1990). Electrodeposition of cobalt from aqueous chloride solutions. J. Electrochem. Soc. *137*, 3418–3423.

Du, X., Sun, X., Zhang, H., Wang, Z., Hao, X., Guan, G., and Abudula, A. (2015). A facile potential-induced in-situ ion removal trick: fabrication of high-selective ion-imprinted film for trivalent yttrium ion separation. Electrochim. Acta *176*, 1313–1323.

Du, X., Zhang, H., Hao, X., Guan, G., and Abudula, A. (2014). Facile preparation of ion-imprinted composite film for selective electrochemical removal of nickel(II) ions. ACS Appl. Mater. Interfaces *6*, 9543–9549.

Elomaa, H., Seisko, S., Junnila, T., Sirviö, T., Wilson, B.P., Aromaa, J., and Lundström, M. (2017). The effect of the redox potential of aqua regia and temperature on the Au, Cu, and Fe dissolution from WPCBs. Recycling *2*, 14.

European Commission (2018). Report on Critical Raw Materials in the Circular Economy.

European Commission (2020). Study on the EU's List of Critical Raw Materials.

Fan, H., and Yip, N.Y. (2019). Elucidating conductivity-permselectivity tradeoffs in electrodialysis and reverse electrodialysis by structure-property analysis of ion-exchange membranes. J. Membr. Sci. *573*, 668–681.

Fleming, C.A. (1992). Hydrometallurgy of precious metals recovery. Hydrometallurgy *30*, 127–162.

Fogg, H.C. (1934). A review of the electrochemistry of gallium. Trans. Electrochem. Soc. *66*, 107.

Fotoohi, B., and Mercier, L. (2014). Recovery of precious metals from ammoniacal thiosulfate solutions by hybrid mesoporous silica: 1-Factors affecting gold adsorption. Separation Purif. Technol. *127*, 84–96.

Frank, A.C., and Sumodjo, P.T.A. (2014). Electrodeposition of cobalt from citrate containing baths. Electrochim. Acta *132*, 75–82.

Gamaethiralalage, J.G., Singh, K., Sahin, S., Yoon, J., Elimelech, M., Suss, M.E., Liang, P., Biesheuvel, P.M., Zornitta, R.L., and de Smet, L.C.P.M. (2021). Recent advances in ion selectivity with capacitive deionization. Energ. Environ. Sci. *14*, 1095–1120.

Gamse, T., Steinkellner, F., Marr, R., Alessi, P., and Kikic, I. (2000). Solubility studies of organic flame retardants in supercritical CO2. Ind. Eng. Chem. Res. *39*, 4888–4890.

Gaustad, G., Krystofik, M., Bustamante, M., and Badami, K. (2018). Circular economy strategies for mitigating critical material supply issues. Resour. Conservat. Recycl. *135*, 24–33.

Gollakota, A.R.K., Gautam, S., and Shu, C.M. (2020). Inconsistencies of e-waste management in developing nations - facts and plausible solutions. J. Environ. Manage *261*, 110234.

Grdeń, M., and Jagiełło, J. (2012). Oxidation of electrodeposited cobalt electrodes in an alkaline electrolyte. J. Solid State Electrochem. *17*, 145–156.

Griškonis, E., Šulčius, A., and Žmuidzinavičienė, N. (2014). Influence of temperature on the properties of Mn coatings electrodeposited from the electrolyte containing Te(VI) additive. J. Appl. Electrochem. *44*, 1117–1125.

Grotheer, M., Alkire, R., and Varjian, R. (2006). Industrial electrolysis and electrochemical engineering. Electrochem. Soc. Interfaces *15*, 52–54.

Gurung, M., Adhikari, B.B., Kawakita, H., Ohto, K., Inoue, K., and Alam, S. (2013). Recovery of gold and silver from spent mobile phones by means of acidothiourea leaching followed by adsorption using biosorbent prepared from persimmon tannin. Hydrometallurgy *133*, 84–93.

Gustafsson, A.M., Bjorefors, F., Steenari, B.M., and Ekberg, C. (2015). Investigation of an electrochemical method for separation of copper, indium, and gallium from pretreated CIGS solar cell waste materials. ScientificWorldJournal *2015*, 494015.

Guyes, E.N., Malka, T., and Suss, M.E. (2019). Enhancing the ion-size-based selectivity of capacitive deionization electrodes. Environ. Sci. Technol. *53*, 8447–8454.

Guyot, E., Seghir, S., Diliberto, S., Lecuire, J.M., and Boulanger, C. (2012). Lithium recovery by electrochemical transfer junction based on intercalation host matrix. Electrochem. Commun. *23*, 29–32.

Guyot, E., Seghir, S., Lecuire, J.M., Boulanger, C., Levi, M.D., Shilina, Y., Dargel, V., and Aurbach, D. (2013). Mo6S8Electrochemical transfer junction for selective extraction of Co2+-ions from their mixture with Ni2+-ions. J. Electrochem. Soc. *160*, A420–A425.

Ha, V.H., Lee, J.-c., Huynh, T.H., Jeong, J., and Pandey, B.D. (2014). Optimizing the thiosulfate leaching of gold from printed circuit boards of discarded mobile phone. Hydrometallurgy *149*, 118–126.

Ha, V.H., Lee, J.-c., Jeong, J., Hai, H.T., and Jha, M.K. (2010). Thiosulfate leaching of gold from waste mobile phones. J. Hazard. Mater. *178*, 1115–1119.

Halli, P., Wilson, B.P., Hailemariam, T., Latostenmaa, P., Yliniemi, K., and Lundström, M. (2019). Electrochemical recovery of tellurium from metallurgical industrial waste. J. Appl. Electrochem. *50*, 1–14.

Harris, M., Meyer, D.M., amp, and Auerswald, K. (1977). The production of electrolytic manganese in South Africa. J. South. Afr. Inst. Min. Metall. *77*, 137–142.

Hartley, J.M., Ip, C.M., Forrest, G.C., Singh, K., Gurman, S.J., Ryder, K.S., Abbott, A.P., and Frisch, G. (2014). EXAFS study into the speciation of metal salts dissolved in ionic liquids and deep eutectic solvents. Inorg. Chem. *53*, 6280–6288.

Haynes, W.M. (2012). CRC Handbook of Chemistry and Physics, 93rd Edition (CRC Press).

He, L.-P., Sun, S.-Y., Mu, Y.-Y., Song, X.-F., and Yu, J.-G. (2016). Recovery of lithium, nickel, cobalt, and manganese from spent lithium-ion batteries using l-tartaric acid as a leachant. ACS Sustain. Chem. Eng. *5*, 714–721.

Hemmatifar, A., Ozbek, N., Halliday, C., and Hatton, T.A. (2020). Electrochemical selective recovery of heavy metal vanadium oxyanion from continuously flowing aqueous streams (ChemSusChem *n/a*).

Hong-Chao, Z., Xi, O., and Abadi, A. (2006). An Environmentally Benign Process Model Development for Printed Circuit Board Recycling. Paper presented at: Proceedings of the 2006 IEEE International Symposium on Electronics and the Environment, 2006.

Hoshino, T. (2015). Innovative lithium recovery technique from seawater by using world-first dialysis with a lithium ionic superconductor. Desalination *359*, 59–63.

Hou, C.-H., and Huang, C.-Y. (2013). A comparative study of electrosorption selectivity of ions by activated carbon electrodes in capacitive deionization. Desalination *314*, 124–129.

Hsu, E., Barmak, K., West, A.C., and Park, A.-H.A. (2019). Advancements in the treatment and processing of electronic waste with sustainability: a review of metal extraction and recovery technologies. Green. Chem. *21*, 919–936.

Hsu, E., Durning, C.J., West, A.C., and Park, A.-H.A. (2020). Enhanced extraction of copper from electronic waste via induced morphological changes using supercritical CO2. Resour. Conservat. Recycl. *168*, 105296.

Huang, S.Y., Fan, C.S., and Hou, C.H. (2014). Electro-enhanced removal of copper ions from aqueous solutions by capacitive deionization. J. Hazard Mater. *278*, 8–15.

Ibañez, A., and Fatás, E. (2005). Mechanical and structural properties of electrodeposited copper and their relation with the electrodeposition parameters. Surf. Coat. Technol. *191*, 7–16.

Işıldar, A., Rene, E.R., van Hullebusch, E.D., and Lens, P.N.L. (2018). Electronic waste as a secondary source of critical metals: management and recovery technologies. Resour. Conservat. Recycl. *135*, 296–312.

Jeon, S., Tabelin, C.B., Takahashi, H., Park, I., Ito, M., and Hiroyoshi, N. (2018). Interference of coexisting copper and aluminum on the ammonium thiosulfate leaching of gold from printed circuit boards of waste mobile phones. Waste Manage *81*, 148–156.

Jin, W., Hu, M., and Hu, J. (2018). Selective and efficient electrochemical recovery of dilute copper and tellurium from acidic chloride solutions. ACS Sustain. Chem. Eng. *6*, 13378–13384.

Jin, W., Su, J., Zheng, S., and Lei, H. (2017). Controlled electrodeposition of uniform copper powder from hydrochloric acid solutions. J. Electrochem. Soc. *164*, D723–D728.

Jin, W., and Zhang, Y. (2020). Sustainable electrochemical extraction of metal resources from waste streams: from removal to recovery. ACS Sustain. Chem. Eng. *8*, 4693–4707.

Jing-ying, L., Xiu-li, X., and Wen-quan, L. (2012). Thiourea leaching gold and silver from the printed circuit boards of waste mobile phones. Waste Manage *32*, 1209–1212.

Joo, H., Kim, S., Kim, S., Choi, M., Kim, S.-H., and Yoon, J. (2020). Pilot-scale demonstration of an electrochemical system for lithium recovery from the desalination concentrate. Environ. Sci. Water Res. Technol. *6*, 290–295.

Kaniyankandy, S., Nuwad, J., Thinaharan, C., Dey, G.K., and Pillai, C.G.S. (2007). Electrodeposition of silver nanodendrites. Nanotechnology *18*, 125610.

Kasper, A.C., Veit, H.M., García-Gabaldón, M., and Herranz, V.P. (2018). Electrochemical study of gold recovery from ammoniacal thiosulfate, simulating the PCBs leaching of mobile phones. Electrochim. Acta *259*, 500–509.

Kim, D.I., Gwak, G., Dorji, P., He, D., Phuntsho, S., Hong, S., and Shon, H. (2017a). Palladium recovery through membrane capacitive deionization from metal plating wastewater. ACS Sustain. Chem. Eng. *6*, 1692–1701.

Kim, T., Gorski, C.A., and Logan, B.E. (2017b). Low energy desalination using battery electrode deionization. Environ. Sci. Technol. Lett. *4*, 444–449.

Kim, K., Cho, H., Jeon, S.H., Lee, S.J., Yoo, C.-Y., Kim, J.-N., Choi, J.W., Yoon, H.C., and Han, J.-I. (2018a). Lithium-mediated ammonia electro-synthesis: effect of CsClO4 on lithium plating efficiency and ammonia synthesis. J. Electrochem. Soc. *165*, F1027–F1031.

Kim, K., Lee, S.J., Kim, D.Y., Yoo, C.Y., Choi, J.W., Kim, J.N., Woo, Y., Yoon, H.C., and Han, J.I. (2018b). Electrochemical synthesis of ammonia from water and nitrogen: A lithium-mediated approach using lithium-ion conducting glass ceramics. ChemSusChem *11*, 120–124.

Kim, S., Kim, J., Kim, S., Lee, J., and Yoon, J. (2018c). Electrochemical lithium recovery and organic pollutant removal from industrial wastewater of a battery recycling plant. Environ. Sci. Water Res. Technol. *4*, 175–182.

Kim, K., Baldaguez Medina, P., Elbert, J., Kayiwa, E., Cusick, R.D., Men, Y., and Su, X. (2020a). Molecular tuning of redox-copolymers for selective electrochemical remediation. Adv. Funct. Mater. *30*, 2004635.

Kim, K., Cotty, S., Elbert, J., Chen, R., Hou, C.H., and Su, X. (2020b). Asymmetric redox-polymer interfaces for electrochemical reactive separations: synergistic capture and conversion of arsenic. Adv. Mater. *32*, e1906877.

Kim, N., Su, X., and Kim, C. (2020c). Electrochemical lithium recovery system through the simultaneous lithium enrichment via sustainable redox reaction. Chem. Eng. J. 127715.

Kim, S., Kang, J.S., Joo, H., Sung, Y.E., and Yoon, J. (2020d). Understanding the behaviors of lambda-MnO2 in electrochemical lithium recovery: key limiting factors and a route to the enhanced performance. Environ. Sci. Technol. *54*, 9044–9051.

King, C.J. (2000). Separation Processes, Introduction. In: Ullmann's Encyclopedia of Industrial Chemistry (John Wiley and Sons, Inc).

Koyama, K., Tanaka, M., and Lee, J.-c. (2006). Copper leaching behavior from waste printed circuit board in ammoniacal alkaline solution. Mater. Trans. *47*, 1788–1792.

Kumari, A., Jha, M.K., and Singh, R.P. (2016). Recovery of metals from pyrolysed PCBs by hydrometallurgical techniques. Hydrometallurgy *165*, 97–105.

Kurachi, A., Matsumiya, M., Tsunashima, K., and Kodama, S. (2012). Electrochemical behavior and electrodeposition of dysprosium in ionic liquids based on phosphonium cations. J. Appl. Electrochem. *42*, 961–968.

Lawagon, C.P., Nisola, G.M., Cuevas, R.A.I., Kim, H., Lee, S.-P., and Chung, W.-J. (2018). Li1−Ni0.33Co1/3Mn1/3O2/Ag for electrochemical lithium recovery from brine. Chem. Eng. J. *348*, 1000–1011.

Lee, M.-S., and Oh, Y.-J. (2005). Chemical Equilibria in a mixed solution of nickel and cobalt chloride. Mater. Trans. *46*, 59–63.

Li, C., Ramasamy, D.L., Sillanpää, M., and Repo, E. (2021). Separation and concentration of rare earth elements from wastewater using electrodialysis technology. Separation Purif. Technol. *254*, 117442.

Li, Y., Zhang, C., Jiang, Y., Wang, T.-J., and Wang, H. (2016). Effects of the hydration ratio on the electrosorption selectivity of ions during capacitive deionization. Desalination *399*, 171–177.

Li, H., Oraby, E., and Eksteen, J. (2020a). Extraction of copper and the co-leaching behaviour of other metals from waste printed circuit boards using alkaline glycine solutions. Resour. Conservat. Recycl. *154*, 104624.

Li, Z.Q., Wu, M.Y., Ding, X.L., Wu, Z.Q., and Xia, X.H. (2020b). Reversible electrochemical tuning of ion sieving in coordination polymers. Anal Chem. *92*, 9172–9178.

Liu, F., Peng, C., Porvali, A., Wang, Z., Wilson, B.P., and Lundström, M. (2019a). Synergistic recovery of valuable metals from spent nickel–metal hydride batteries and lithium-ion batteries. ACS Sustain. Chem. Eng. *7*, 16103–16111.

Liu, X., Wu, J., and Wang, J. (2019b). Electro-enhanced removal of cobalt ions from aqueous solution by capacitive deionization. Sci. Total Environ. *697*, 134144.

Liu, C., Hsu, P.-C., Xie, J., Zhao, J., Wu, T., Wang, H., Liu, W., Zhang, J., Chu, S., and Cui, Y. (2017). A half-wave rectified alternating current electrochemical method for uranium extraction from seawater. Nat. Energy *2*, 17007.

Liu, Y., Ke, X., Wu, X., Ke, C., Chen, R., Chen, X., Zheng, X., Jin, Y., and Van der Bruggen, B. (2020). Simultaneous removal of Trivalent chromium and Hexavalent chromium from soil using a modified bipolar membrane electrodialysis system. Environ. Sci. Technol. *54*, 13304–13313.

Lodermeyer, J., Multerer, M., Zistler, M., Jordan, S., Gores, H.J., Kipferl, W., Diaconu, E., Sperl, M., and Bayreuther, G. (2006). Electroplating of dysprosium, electrochemical investigations, and study of magnetic properties. J. Electrochem. Soc. *153*, C242–C248.

Long, X., Chen, R., Tan, J., Lu, Y., Wang, J., Huang, T., and Lei, Q. (2020). Electrochemical recovery of cobalt using nanoparticles film of copper hexacyanoferrates from aqueous solution. J. Hazard Mater. *384*, 121252.

Lu, J., Dreisinger, D., and Glück, T. (2014). Manganese electrodeposition — a literature review. Hydrometallurgy *141*, 105–116.

Maarof, H.I., Daud, W.M.A.W., and Aroua, M.K. (2017). Recent trends in removal and recovery of heavy metals from wastewater by electrochemical technologies. Rev. Chem. Eng. *33*, 359–386.

Maguyon, M.C.C., Alfafara, C.G., Migo, V.P., Movillon, J.L., and Rebancos, C.M. (2012). Recovery of copper from spent solid printed-

circuit-board (PCB) wastes of a PCB manufacturing facility by two-step sequential acid extraction and electrochemical deposition. J. Environ. Sci. Manag. *15*, 17–27.

Martins, R., Britto-Costa, P.H., and Ruotolo, L.A. (2012). Removal of toxic metals from aqueous effluents by electrodeposition in a spouted bed electrochemical reactor. Environ. Technol. *33*, 1123–1131.

Mashtalir, O., Nguyen, M., Bodoin, E., Swonger, L., and O'Brien, S.P. (2018). High-purity lithium metal films from aqueous mineral solutions. ACS Omega *3*, 181–187.

Mecucci, A., and Scott, K. (2002). Leaching and electrochemical recovery of copper, lead and tin from scrap printed circuit boards. J. Chem. Technol. Biot *77*, 449–457.

Mollah, M.Y., Morkovsky, P., Gomes, J.A., Kesmez, M., Parga, J., and Cocke, D.L. (2004). Fundamentals, present and future perspectives of electrocoagulation. J. Hazard Mater. *114*, 199–210.

Montero, R., Guevara, A., and Torre, E.D.L. (2012). Recovery of Gold, Silver, Copper and Niobium from Printed Circuit Boards Using Leaching Column Technique. J. Earth Sci. Eng. *2*, 590–595.

Murthy, Z.V.P., and Parmar, S. (2011). Removal of strontium by electrocoagulation using stainless steel and aluminum electrodes. Desalination *282*, 63–67.

Neto, I.F.F., Sousa, C.A., Brito, M.S.C.A., Futuro, A.M., and Soares, H.M.V.M. (2016). A simple and nearly-closed cycle process for recycling copper with high purity from end life printed circuit boards. Separation Purif. Technol. *164*, 19–27.

Nie, X.-Y., Sun, S.-Y., Sun, Z., Song, X., and Yu, J.-G. (2017). Ion-fractionation of lithium ions from magnesium ions by electrodialysis using monovalent selective ion-exchange membranes. Desalination *403*, 128–135.

Niu, J., Yan, W., Du, J., Hao, X., Wang, F., Wang, Z., and Guan, G. (2020). An electrically switched ion exchange film with molecular coupling synergistically-driven ability for recovery of Ag+ ions from wastewater. Chem. Eng. J. *389*, 124498.

O'Connor, M.P., Coulthard, R.M., and Plata, D.L. (2018). Electrochemical deposition for the separation and recovery of metals using carbon nanotube-enabled filters. Environ. Sci. Water Res. Technol. *4*, 58–66.

Oh, C.J., Lee, S.O., Yang, H.S., Ha, T.J., and Kim, M.J. (2012). Selective leaching of valuable metals from waste printed circuit boards. J. Air Waste Manag. Assoc. *53*, 897–902.

Oriňáková, R., Turoňová, A., Kladeková, D., Gálová, M., and Smith, R.M. (2006). Recent developments in the electrodeposition of nickel and some nickel-based alloys. J. Appl. Electrochem. *36*, 957–972.

Padhy, S.K., Patnaik, P., Tripathy, B.C., Ghosh, M.K., and Bhattacharya, I.N. (2016). Electrodeposition of manganese metal from sulphate solutions in the presence of sodium octyl sulphate. Hydrometallurgy *165*, 73–80.

Pasta, M., Battistel, A., and La Mantia, F. (2012). Batteries for lithium recovery from brines. Energy Environ. Sci. *5*, 9487.

Paul Chen, J., and Lim, L.L. (2005). Recovery of precious metals by an electrochemical deposition method. Chemosphere *60*, 1384–1392.

Peng, P., and Park, A.-H.A. (2020). Supercritical CO2-induced alteration of a polymer–metal matrix and selective extraction of valuable metals from waste printed circuit boards. Green. Chem. *22*, 7080–7092.

Peng, Q., Liu, L., Luo, Y., Zhang, Y., Tan, W., Liu, F., Suib, S.L., and Qiu, G. (2016). Cadmium removal from aqueous solution by a deionization Supercapacitor with a birnessite electrode. ACS Appl. Mater. Interfaces *8*, 34405–34413.

Petter, P.M.H., Veit, H.M., and Bernardes, A.M. (2015). Leaching of gold and silver from printed circuit board of mobile phones. Rem: Revista Escola de Minas *68*, 61–68.

Prakash, V., Sun, Z.H.I., Sietsma, J., and Yang, Y. (2016). Simultaneous electrochemical recovery of rare earth elements and iron from magnet scrap. In Rare Earths Industry, pp. 335–346.

Rassat, S.D., Sukamto, J.H., Orth, R.J., Lilga, M.A., and Hallen, R.T. (1999). Development of an electrically switched ion exchange process for selective ion separations. Separation Purif. Technol. *15*, 207–222.

Raub, C. (1993). 23 - the history of electroplating. In Metal Plating and Patination, S.L. Niece and P. Craddock, eds. (Butterworth-Heinemann), pp. 284–290.

Ren, M., Ning, P., Xu, J., Qu, G., and Xie, R. (2018). Concentration and treatment of ceric ammonium nitrate wastewater by integrated electrodialysis-vacuum membrane distillation process. Chem. Eng. J. *351*, 721–731.

Reyes Cruz, V., Oropeza, M.T., González, I., and Ponce-De-León, C. (2002). Electrochemical recovery of silver from cyanide leaching solutions. J. Appl. Electrochem. *32*, 473–479.

Sadyrbaeva, T.Z. (2015). Separation of cobalt(II) from nickel(II) by a hybrid liquid membrane–electrodialysis process using anion exchange carriers. Desalination *365*, 167–175.

Sanchez-Cupido, L., Pringle, J.M., Siriwardana, A.L., Unzurrunzaga, A., Hilder, M., Forsyth, M., and Pozo-Gonzalo, C. (2019). Water-facilitated electrodeposition of neodymium in a phosphonium-based ionic liquid. J. Phys. Chem. Lett. *10*, 289–294.

Sandell, E.B. (1968). Meaning of the term "separation factor. Anal. Chem. *40*, 834–835.

Santos, V.E.O., Celante, V.G., Lelis, M.F.F., and Freitas, M.B.J.G. (2012). Chemical and electrochemical recycling of the nickel, cobalt, zinc and manganese from the positives electrodes of spent Ni–MH batteries from mobile phones. J. Power Sourc. *218*, 435–444.

Scott, K. (1981). Metal recovery using a moving-bed electrode. J. Appl. Electrochem. *11*, 339–346.

Seader, J.D., Henley, E.J., and Roper, D.K. (1998). Separation Process Principles, *Vol 25* (wiley New York).

Semerci, N., Kunt, B., and Calli, B. (2019). Phosphorus recovery from sewage sludge ash with bioleaching and electrodialysis. Int. Biodeterior. Biodegradation *144*, 104739.

Sethurajan, M., van Hullebusch, E.D., Fontana, D., Akcil, A., Deveci, H., Batinic, B., Leal, J.P., Gasche, T.A., Ali Kucuker, M., Kuchta, K., et al. (2019). Recent advances on hydrometallurgical recovery of critical and precious elements from end of life electronic wastes - a review. Crit. Rev. Environ. Sci. Technol. *49*, 212–275.

Shi, D., Cui, B., Li, L., Peng, X., Zhang, L., and Zhang, Y. (2019a). Lithium extraction from low-grade salt lake brine with ultrahigh Mg/Li ratio using TBP – kerosene – FeCl3 system. Separation Purif. Technol. *211*, 303–309.

Shi, W., Liu, X., Ye, C., Cao, X., Gao, C., and Shen, J. (2019b). Efficient lithium extraction by membrane capacitive deionization incorporated with monovalent selective cation exchange membrane. Separation Purif. Technol. *210*, 885–890.

Shi, W., Nie, P., Shang, X., Yang, J., Xie, Z., Xu, R., and Liu, J. (2019c). Berlin green-based battery deionization-highly selective potassium recovery in seawater. Electrochim. Acta *310*, 104–112.

Silvas, F.P.C., Jiménez Correa, M.M., Caldas, M.P.K., de Moraes, V.T., Espinosa, D.C.R., and Tenório, J.A.S. (2015). Printed circuit board recycling: physical processing and copper extraction by selective leaching. Waste Manage *46*, 503–510.

Singh, K., Bouwmeester, H.J.M., de Smet, L.C.P.M., Bazant, M.Z., and Biesheuvel, P.M. (2018). Theory of water desalination with intercalation materials. Phys. Rev. Appl. *9*, 064036.

Sole, K.C. (2018). The evolution of cobalt–nickel separation and purification technologies: fifty years of solvent extraction and ion exchange. In Extraction 2018, pp. 1167–1191.

Son, M., Aronson, B.L., Yang, W., Gorski, C.A., and Logan, B.E. (2020). Recovery of ammonium and phosphate using battery deionization in a background electrolyte. Environ. Sci. Water Res. Technol. *6*, 1688–1696.

Spitzer, M., and Bertazzoli, R. (2004). Selective electrochemical recovery of gold and silver from cyanide aqueous effluents using titanium and vitreous carbon cathodes. Hydrometallurgy *74*, 233–242.

Srimuk, P., Lee, J., Fleischmann, S., Aslan, M., Kim, C., and Presser, V. (2018). Potential-dependent, switchable ion selectivity in aqueous media using titanium disulfide. ChemSusChem *11*, 2091–2100.

Srimuk, P., Su, X., Yoon, J., Aurbach, D., and Presser, V. (2020). Charge-transfer materials for electrochemical water desalination, ion separation and the recovery of elements. Nat. Rev. Mater. *5*, 517–538.

Strathmann, H. (2010). Electrodialysis, a mature technology with a multitude of new applications. Desalination *264*, 268–288.

Su, X. (2020a). Electrochemical interfaces for chemical and biomolecular separations. Curr. Opin. Colloid Interface Sci. *46*, 77–93.

Su, X. (2020b). Electrochemical separations for metal recycling. Electrochem. Soc. Interf. *29*, 55–61.

Su, X., and Hatton, T.A. (2016). Electrosorption. In Kirk-Othmer Encyclopedia of Chemical Technology (John Wiley & Sons), pp. 1–11.

Su, X., and Hatton, T.A. (2017a). Electrosorption at functional interfaces: from molecular-level interactions to electrochemical cell design. Phys. Chem. Chem. Phys. *19*, 23570–23584.

Su, X., and Hatton, T.A. (2017b). Redox-electrodes for selective electrochemical separations. Adv. Colloid. Interface Sci. *244*, 6–20.

Su, X., Kulik, H.J., Jamison, T.F., and Hatton, T.A. (2016). Anion-selective redox electrodes: electrochemically mediated separation with heterogeneous Organometallic interfaces. Adv. Funct. Mater. *26*, 3394–3404.

Su, X., Kushima, A., Halliday, C., Zhou, J., Li, J., and Hatton, T.A. (2018). Electrochemically-mediated selective capture of heavy metal chromium and arsenic oxyanions from water. Nat. Commun. *9*, 4701.

Su, X., Tan, K.-J., Elbert, J., Rüttiger, C., Gallei, M., Jamison, T.F., and Hatton, T.A. (2017). Asymmetric Faradaic systems for selective electrochemical separations. Energy Environ. Sci. *10*, 1272–1283.

Sun, B., Hao, X.G., Wang, Z.D., Guan, G.Q., Zhang, Z.L., Li, Y.B., and Liu, S.B. (2012). Separation of low concentration of cesium ion from wastewater by electrochemically switched ion exchange method: experimental adsorption kinetics analysis. J. Hazard Mater. *233-234*, 177–183.

Sun, X., Zhang, X., Ma, Q., Guan, X., Wang, W., and Luo, J. (2020). Revisiting the electroplating process for lithium-metal anodes for lithium-metal batteries. Angew. Chem. Int. Ed. *59*, 6665–6674.

Sun, Y., Tian, X., He, B., Yang, C., Pi, Z., Wang, Y., and Zhang, S. (2011). Studies of the reduction mechanism of selenium dioxide and its impact on the microstructure of manganese electrodeposit. Electrochim. Acta *56*, 8305–8310.

Sun, Z., Xiao, Y., Sietsma, J., Agterhuis, H., and Yang, Y. (2015). A cleaner process for selective recovery of valuable metals from electronic waste of complex mixtures of end-of-life electronic products. Environ. Sci. Technol. *49*, 7981–7988.

Tan, K.-J., Su, X., and Hatton, T.A. (2020). An asymmetric iron-based redox-active system for electrochemical separation of ions in aqueous media. Adv. Funct. Mater. *30*, 1910363.

Tran, M.K., Rodrigues, M.-T.F., Kato, K., Babu, G., and Ajayan, P.M. (2019). Deep eutectic solvents for cathode recycling of Li-ion batteries. Nat. Energy *4*, 339–345.

Tripathi, A., Kumar, M., Sau, D.C., Agrawal, A., Chakravarty, S., and Mankhand, T.R. (2012). Leaching of gold from the waste mobile phone printed circuit boards (PCBs) with ammonium Thiosulphate. Int. J. Metall. Eng. *1*, 17–21.

Tunsu, C., and Retegan, T. (2016). Hydrometallurgical processes for the recovery of metals from WEEE. WEEE Recycling, pp. 139–175.

Tzanetakis, N., and Scott, K. (2004). Recycling of nickel–metal hydride batteries. II: electrochemical deposition of cobalt and nickel. J. Chem. Technol. Biotechnol. *79*, 927–934.

U.S. Department of Energy (2011). Critical Materials Strategy.

Wang, J., Yang, S., Long, X., Li, Z., Tan, J., Wang, X., and Chen, R. (2020). Electrochemical recovery of low concentrated platinum (Pt) on nickel hexacyanoferrate nanoparticles film. J. Taiwan Inst. Chem. Eng. *111*, 246–251.

Wang, Y., and Zhou, H. (2010). A lithium-air battery with a potential to continuously reduce O2 from air for delivering energy. J. Power Sourc. *195*, 358–361.

Wang, P., Du, X., Chen, T., Hao, X., Abudula, A., Tang, K., and Guan, G. (2019a). A novel electroactive PPy/HKUST-1 composite film-coated electrode for the selective recovery of lithium ions with low concentrations in aqueous solutions. Electrochim. Acta *306*, 35–44.

Wang, Z., Du, J., Yan, W., Zhang, W., Niu, J., Wu, A., Hao, X., and Guan, G. (2019b). A potential-responsive affinity-controlling 2-2′-dithiodibenzoic acid/polyaniline hybrid film with high ion exchange capability and selectivity to cadmium ions. Electrochim. Acta *319*, 615–624.

Weidlich, C., Mangold, K.M., and Jüttner, K. (2005). Continuous ion exchange process based on polypyrrole as an electrochemically switchable ion exchanger. Electrochim. Acta *50*, 5247–5254.

Xiao, Y., Yang, Y., van den Berg, J., Sietsma, J., Agterhuis, H., Visser, G., and Bol, D. (2013). Hydrometallurgical recovery of copper from complex mixtures of end-of-life shredded ICT products. Hydrometallurgy *140*, 128–134.

Xu, X., Sturm, S., Samardzija, Z., Scancar, J., Markovic, K., and Zuzek Rozman, K. (2020). A facile method for the simultaneous recovery of rare-earth elements and transition metals from Nd–Fe–B magnets. Green. Chem. *22*, 1105–1112.

Yang, H., Liu, J., and Yang, J. (2011). Leaching copper from shredded particles of waste printed circuit boards. J. Hazard. Mater. *187*, 393–400.

Yang, X., Liu, L., Tan, W., Qiu, G., and Liu, F. (2018). High-performance Cu2+ adsorption of birnessite using electrochemically controlled redox reactions. J. Hazard. Mater. *354*, 107–115.

Yang, Y.-s., Zhang, M.-l., Han, W., Sun, P.-y., Liu, B., Jiang, H.-l., Jiang, T., Peng, S.-m., Li, M., Ye, K., et al. (2014). Selective electrodeposition of dysprosium in LiCl-KCl-GdCl3-DyCl3 melts at magnesium electrodes: application to separation of nuclear wastes. Electrochim. Acta *118*, 150–156.

Yoon, H., Lee, J., Kim, S., and Yoon, J. (2019). Review of concepts and applications of electrochemical ion separation (EIONS) process. Separation Purif. Technol. *215*, 190–207.

You, Y.H., Gu, C.D., Wang, X.L., and Tu, J.P. (2012). Electrodeposition of Ni–Co alloys from a deep eutectic solvent. Surf. Coat. Technol. *206*, 3632–3638.

Yousefzadeh, S., Yaghmaeian, K., Mahvi, A.H., Nasseri, S., Alavi, N., and Nabizadeh, R. (2020). Comparative analysis of hydrometallurgical methods for the recovery of Cu from circuit boards: optimization using response surface and selection of the best technique by two-step fuzzy AHP-TOPSIS method. J. Clean. Prod. *249*, 119401.

Yu, Y. (2017). Study on electrochemistry and nucleation process of nickel electrodeposition. Int. J. Electrochem. Sci. 485–495.

Zeng, X., Mathews, J.A., and Li, J. (2018). Urban mining of E-waste is becoming more cost-effective than virgin mining. Environ. Sci. Technol. *52*, 4835–4841.